

Article

Double Beta Decay to Excited States of Daughter Nuclei

Pierluigi Belli ^{1,2,*} , Rita Bernabei ^{1,2} , Fabio Cappella ^{3,4} , Vincenzo Caracciolo ^{1,2,5} ,
Riccardo Cerulli ^{1,2} , Antonella Incicchitti ^{3,4}  and Vittorio Merlo ^{1,2} 

¹ INFN, sezione di Roma Tor Vergata, I-00133 Rome, Italy; rita.bernabei@roma2.infn.it (R.B.); vincenzo.caracciolo@roma2.infn.it (V.C.); riccardo.cerulli@roma2.infn.it (R.C.); vittorio.merlo@roma2.infn.it (V.M.)

² Dipartimento di Fisica, Università di Roma “Tor Vergata”, I-00133 Rome, Italy

³ INFN, sezione di Roma, I-00185 Rome, Italy; fabio.cappella@roma1.infn.it (F.C.); antonella.incicchitti@roma1.infn.it (A.I.)

⁴ Dipartimento di Fisica, Università di Roma “La Sapienza”, I-00185 Rome, Italy

⁵ INFN, Laboratori Nazionali del Gran Sasso, 67100 Assergi (AQ), Italy

* Correspondence: pierluigi.belli@roma2.infn.it

Received: 17 November 2020; Accepted: 8 December 2020; Published: 13 December 2020



Abstract: In this paper we review results obtained in the searches of double beta decays to excited states of the daughter nuclei and illustrate the related experimental techniques. In particular, we describe in some detail the only two cases in which the transition has been observed; that is the $2\beta^-(0^+ \rightarrow 0_1^+)$ decay of ^{100}Mo and ^{150}Nd nuclides. Moreover, the most significant results in terms of lower limits on the half-life are also summarized.

Keywords: double beta decay; scintillation detector; low background experiment

1. Introduction

In 1935 Maria Goeppert-Mayer described a second-order weak-interaction process: the double beta ($\beta\beta$) decay¹, a transition between isobaric nuclei where two neutrons simultaneously decay into protons ($2\beta^-$) [1]; this process can occur in neutron-rich nuclei. In proton-rich nuclei, up to three competing processes can be kinematically available—the double β^+ emission ($2\beta^+$), the single β^+ emission plus single electron capture ($\epsilon\beta^+$), and double electron capture (2ϵ). The $\beta\beta$ decay is strongly suppressed and can only be observed in those isotopes where single beta decay is forbidden. The two neutrino $\beta\beta$ decay has been observed in several nuclei; however the $\beta\beta$ decay processes discussed by Furry in 1939, namely the neutrinoless double beta decay ($0\nu\beta\beta$) [2], is requiring further efforts in various isotopes. The $\beta\beta$ decay modes without emission of neutrinos would be highly relevant in proving the existence of a process violating the conservation of the total lepton number and of the (baryon-lepton) number quantity (B-L). The detection of a process violating (B-L) would have implications in theories trying to explain matter and anti-matter asymmetry in the Universe. The $0\nu\beta\beta$ decay mode would prove the non-conservation of the lepton number and would be a key tool to probe if the neutrino—contrary to all the other known fermions—is a Majorana particle, that is, it coincides with its own anti-particle. A fundamental step toward sensitive investigations on neutrino-less $\beta\beta$ decay modes is the unambiguous and precise measurement of the two-neutrino $\beta\beta$ decay ones.

¹ Throughout the paper the wording $\beta\beta$ indicate the generic double beta decay, with neutrinos or neutrino-less. Where not specified, it includes the cases with electrons emission, $2\beta^-$, with positrons emission, $2\beta^+$, the single positron emission plus single electron capture, $\epsilon\beta^+$, and the double electron capture, 2ϵ .

The latter process is allowed in the Standard Model of particle physics (SM) although predicted to be extremely rare; these predictions use many-body techniques and nuclear models similar to those applied for $0\nu\beta\beta$ decay; thus, measurements of $2\nu\beta\beta$ decay are also relevant for interpreting $0\nu\beta\beta$ decay results. In conclusion, the $\beta\beta$ decay is among the rarest processes in nature and offers an ideal benchmark to study atomic physics, nuclear physics, and physics beyond the Standard Model.

Another way to approach the investigation of $\beta\beta$ decay processes is to study decays where the daughter nucleus is left in an excited state; then, the excited state will decay to the ground state emitting gamma rays. However, excited-state $\beta\beta$ decay transitions have a smaller Q -value than the ground state-ground state transitions and, thus, a longer half-life. Nevertheless, more research on such transitions is needed from both the experimental and the theoretical sides.

In the following we will introduce and discuss several experimental results in the searches for $\beta\beta$ decay processes to excited states of daughter nuclei with some perspectives.

2. Double Beta Decay to Excited States of Daughter Nuclei

Studies on $\beta\beta$ decay to excited levels provide supplementary information about the $\beta\beta$ decay of the parent nuclide. Further information on dynamics of the $\beta\beta$ decays can also be inferred by the $2\beta^+$, $\varepsilon\beta^+$, and 2ε processes both to the ground and the excited states. Despite the lower decay probability of the $2\beta^+$ and $\varepsilon\beta^+$ processes with respect to that of the $2\beta^-$ processes (due to the suppression of the phase space factor), the investigations of these decay modes either to the ground or to the excited states can also strongly contribute to clarify the mechanism of the $0\nu2\beta^-$ decay [3]. In addition, the investigations of the $0\nu2\varepsilon$ processes to excited levels of daughter nuclei can profit of the possibility of a resonant enhancement of the capture rate by several orders of magnitude in case the initial and final states are energetically degenerate [4–10]. In such a case, the resonant effect can provide a sensitivity of the $0\nu2\varepsilon$ process approaching the case of $0\nu2\beta^-$ decay. The effect was pointed out by R.G. Winter [4] in 1955 and further stressed by few other authors in the 1980s [5,9]. The key parameter for the resonant $0\nu2\varepsilon$ processes is the degeneracy parameter, δ , equal to the mass difference of the parent and the daughter atoms. The maximum enhancement is obtained for $\delta = 0$. However, it has been demonstrated (see for example Reference [7]) that even for $\delta \approx 10$ keV an enhancement of a factor 10^6 can be achieved, leading to a renewed interest in these double beta decay processes.

The $\beta\beta$ decay to excited levels of daughter nuclei provides a very clear signature; in addition to the two electrons/positrons either one or two/more photons due to nuclear de-excitation with well identified energies are present. Moreover, for $2\beta^+$, and $\varepsilon\beta^+$ decay 511 keV γ -rays from positrons annihilation are present as well, while for $\varepsilon\beta^+$, and 2ε characteristic X-rays can improve the detection efficiency. All this can offer the possibility to study such decays by coincidence techniques.

Thus, since the beginning several different techniques have been used, such as:

- the *source = detector* technique using low-background detectors containing the nuclides of interest. Germanium detectors, bolometers, scintillation detectors, ionization detectors, even enriched in particular isotopes, have been used.
- the *coincidence technique* between a low-background detector containing the nuclides of interest and other detectors, as either scintillators or HP-Ge detectors.
- the *source \neq detector* technique by measuring either the gamma emission of a pure sample of material containing the nuclides of interest mostly by means of HP-Ge detectors and/or the electrons/positrons coming out of the source.

An important issue, that is common to all these different experimental techniques, is the use of low background set-ups placed in underground laboratories (although some experimental results have been obtained in shallow deep sites). The cores of the experiments are well shielded by the environmental radioactivity through heavy either passive or active shields. The radon present in trace in the atmosphere in proximity of the experimental site is generally removed by suitable sealed radon removal systems. In addition, the detectors and all their components, and the external source materials

if present are carefully checked, cleaned and in some cases purified for low-radioactivity (see also later). For a discussion of these techniques see, for example, Reference [11].

Since the beginning, the $\beta\beta$ decay to the excited levels of the daughter nuclei was studied as a by-product of the experiments searching for $\beta\beta$ decay to ground states. The first experimental study on $\beta\beta$ decay to the excited levels of the daughter nuclei was reported in 1977 in the search for $\beta\beta$ decay of ^{76}Ge [12]. As a by-product of this experiment the double beta decay of ^{76}Ge to the first excited state of ^{76}Se was also considered [12]. Other studies were performed few years later in Reference [13] looking for the de-excitation gamma-rays following the double beta decay processes through a 130 cm³ Ge(Li) detector at sea level and in the Mont Blanc tunnel. Commercial purified samples of neodymium, nickel, and molybdenum have been placed in the proximity of the sensitive zone of the Ge(Li) detector. These measurements allowed—in addition to the study of the $\beta\beta$ decay of ^{76}Ge present in the natural composition of the germanium itself of the detector—the first study of the $\beta\beta$ decay of ^{148}Nd , ^{150}Nd , ^{58}Ni , ^{92}Mo , and ^{100}Mo to the excited levels of the daughter nuclei. No evidence was found for the processes searched for and limits on the half-life, $T_{1/2}$, were set at level of 10^{21} yr for ^{76}Ge transitions and at level of $(10^{18} - 4 \times 10^{21})$ yr for the other isotopes [13].

The merit of such experiments was the opening of the investigation on the $\beta\beta$ decay to the excited levels of daughter nuclei. In those years the development and the use of low-background High Purity Germanium (HP-Ge) detectors in underground facilities (see, for example, Reference [14]) were pointed out as an interesting possibility to detect the gamma rays produced in the de-excitation of the nuclear levels after a $\beta\beta$ decay to excited levels of daughter nuclei. In particular, it was shown that this process could be detected in three nuclei [15]: ^{96}Zr , ^{100}Mo and ^{150}Nd . The corresponding half-lives were evaluated at that time to be of order of $(10^{20} - 2 \times 10^{21})$ yr [15], reachable by the low-background installations available at that time.

Later on, the $2\beta^-$ decay of ^{100}Mo to the 0_1^+ excited level at 1130.32 keV of ^{100}Ru was observed [16]. A 956 g sample of molybdenum powder enriched to 98.5% in ^{100}Mo was exposed in a low-background germanium detector; excesses of (66 ± 22) and (67 ± 19) events were measured in the energy regions of the expected gamma rays: 539.5 keV and 590.8 keV, respectively [16]. Other experiments confirmed this result, improving the experimental sensitivity (see Section 3).

Ten years later, in 2004 there was the first observation of the $2\beta^-$ decay of ^{150}Nd to the 0_1^+ excited level at 740.46 keV of ^{150}Sm [17]. About 3 kg of neodymium oxide powder was measured with a HP-Ge detector; excesses of (86 ± 28) and (100 ± 25) counts were measured in the energy regions of the expected gamma rays: 334.0 keV and 406.5 keV, respectively [17]. Since then, other results with improved sensitivity were achieved; they are summarized in Section 4.

Since the first works in the 1980s, the sensitivities to double beta decay experiments improved significantly and new limits for many nuclei and different modes of decay to the excited states of daughter nuclei were established. Some of them will be quoted and summarized in Section 5. Examples of the reached sensitivities for the double beta decay channels to excited levels in germanium detectors, bolometers and scintillators will be described in Sections 5.1–5.3, respectively. The technique of the passive source using gamma spectrometers, as low-background germanium detectors, will be summarize in Section 5.4.

3. Positive Results from ^{100}Mo $2\beta^-$ Decay to the 0_1^+ Excited Level

The ^{100}Mo is one of the most interesting and most investigated isotopes for $\beta\beta$ decay searches among all the 35 naturally occurring $2\beta^-$ candidates due to: (i) its rather high natural abundance: $\delta = 9.744(65)\%$ [18]; (ii) the possibility to obtain isotopically enriched material using the comparatively inexpensive ultra-speed centrifuge technology; (iii) the high energy release of $Q_{\beta\beta} = 3034.36(17)$ keV [19] which defines a large phase space integral of the decay and, thus, a relatively high probability of $\beta\beta$ processes. The allowed $2\nu 2\beta^-$ decay to the ground state of ^{100}Ru was observed in several direct experiments. The most accurate value comes from the recent experiment CUPID-Mo using lithium molybdate ($\text{Li}_2^{100}\text{MoO}_4$) scintillating bolometers: $T_{1/2}^{2\nu} = (7.12_{-0.14}^{+0.18}(\text{stat.}) \pm 0.10(\text{syst.})) \times 10^{18}$ yr [20].

In addition to the transition to the ground state, the $2\nu 2\beta^-$ decay of ^{100}Mo was registered also for the transition to the first excited 0_1^+ level of ^{100}Ru (see Figure 1).

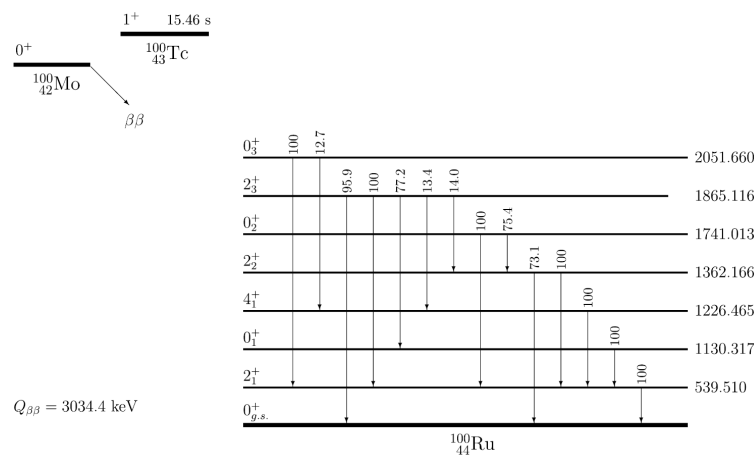


Figure 1. Scheme of $2\beta^-$ decay of ^{100}Mo to the ground state and to the first excited levels of ^{100}Ru (reprinted from Reference [21] with permission from Elsevier). The energies of the levels and the relative main branching ratios are taken from Reference [22].

The half-life of the $^{100}\text{Mo} \rightarrow ^{100}\text{Ru}(0_1^+)$ decay was measured in several experiments [16,21,23–28] in the range of $(5.5 - 9.3) \times 10^{20}$ yr, with a recommended value: $(6.7^{+0.5}_{-0.4}) \times 10^{20}$ yr [29] (see later). Many of these experiments also searched for ^{100}Mo $2\beta^-$ decay to other excited levels of ^{100}Ru [16,21,23,25–27]. The best experimental lower limits on the half-lives of these processes are reported in Table 1.

Table 1. Experimental results on $T_{1/2}$ of the $2\beta^-$ decay of ^{100}Mo to the excited states of ^{100}Ru . All limits are given at 90% C.L.

Transition	Level (keV)	$Q_{\beta\beta}$ (keV)	$T_{1/2}$ (10^{20} yr)	Ref
$0^+ \rightarrow 2_1^+$	539.5	2494.9	>25	[21]
$0^+ \rightarrow 0_1^+$	1130.3	1904.0	$6.7^{+0.5}_{-0.4}$	[29]
$0^+ \rightarrow 2_2^+$	1362.2	1672.2	>108	[21]
$0^+ \rightarrow 0_2^+$	1741.0	1293.3	>48	[27]
$0^+ \rightarrow 2_3^+$	1865.1	1169.2	>49	[21]
$0^+ \rightarrow 0_3^+$	2051.7	982.7	>43	[21]
$0^+ \rightarrow 0_4^+$	2387.4	647.0	>40	[27]

In the following of this section, the experiments which obtained a positive result in the search for $2\beta^-$ decay of ^{100}Mo to the first excited 0_1^+ level of ^{100}Ru will be briefly reviewed.

The first search for this transition was performed in 1982 and only a lower limit on the half-life $T_{1/2} > 0.2 \times 10^{19}$ yr (90% C.L.) was obtained [13]. Afterwards, this decay mode was positively identified by an experiment located in the Soudan mine in Minnesota (2090 m w.e. depth) [16]. A sample of 956 g of powdered molybdenum metal, enriched to $(98.468 \pm 0.009)\%$ in ^{100}Mo and contained in a lucite Marinelli beaker, was measured using a low-background 114 cm³ HP-Ge detector assembled in a cryostat of low-background copper components housed in a large bulk shield of ordinary lead having an inner lining 5 cm thick 150-yr-old lead (see Figure 2 (left)). The bulk shield was sealed and fluxed with nitrogen boil-off gas to mitigate radon in the shield. The energy spectrum obtained in 415.43 days of counting is shown in Figure 2, right. The two expected peaks from the $2\beta^-$ decay de-excitation were observed: (66 ± 22) counts for the 539.5 keV peak and (67 ± 19) counts for the 590.8 keV peak. The corresponding half-life was calculated to be $T_{1/2} = (6.1^{+1.8}_{-1.1}) \times 10^{20}$ yr [16].

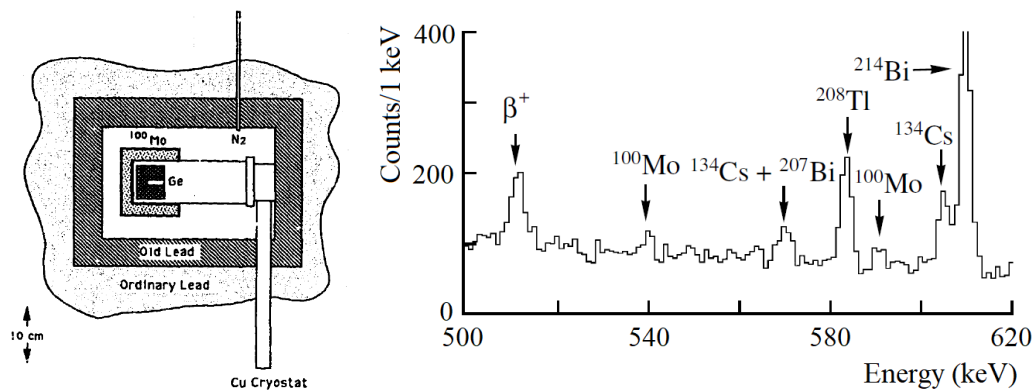


Figure 2. (left) Scheme of the setup used in the Soudan experiment. (right) Energy spectrum obtained by the Soudan experiment over 415.43 days in the energy range corresponding to the $2\beta^-$ decay of ^{100}Mo to the 0_1^+ state of ^{100}Ru at 1130.3 keV, which is accompanied by two γ quanta (539.5 keV and 590.8 keV). Reprinted from Reference [16] with permission from Elsevier.

After a null result in Reference [30] not consistent with the Soudan experiment, a new positive result for $2\beta^-$ decay of ^{100}Mo to the 0_1^+ level of ^{100}Ru was obtained few years later, in 1999 [23]. A set of 17 different ^{100}Mo enriched metallic powder samples (107–1005 g, enriched to 95.1–99.3%) was measured by using low-background HP-Ge detectors. The total spectrum was obtained from the data collected in 17 measurements with the different samples (142–1599 h measuring time). Small peaks were found in the regions of interest with (86 ± 25) events at 539.5 keV and (67 ± 23) events at 590.8 keV. The half-life of $T_{1/2} = (9.3^{+2.8}_{-1.7}) \times 10^{20}$ yr was deduced from the summed γ -ray spectrum, with an additional systematic error estimated to be approximately 15% [23].

Another positive result was then obtained by the TUNL-ITEP experiment in 2000 [24] and with improved sensitivity in the following years [25,27]. The experiment was performed at a shallow depth in the basement of the Physics Department of Duke University (USA). A novel method was used, with two HP-Ge detectors in a coincidence scheme, where two separate detectors simultaneously detect the two emitted γ rays (590.8 and 539.5 keV) from the $2\nu 2\beta^- (0^+ \rightarrow 0_1^+)$ decay of ^{100}Mo . In particular, a disk sample of enriched Mo (1.05 kg mass, 106 mm diameter, 11 mm thickness and enriched to 98.4% in ^{100}Mo) was sandwiched between the front faces of two large HP-Ge detectors that work in the coincidence regime (see Figure 3 (left)). The HP-Ge detectors, 85 mm in diameter by 50 mm in length, were inserted in a NaI(Tl) annulus used as an active veto. Plastic plates (10 cm thickness) on either side of the apparatus acted as a veto for the regions which are not covered by the NaI(Tl) annulus. The entire apparatus was surrounded by a passive shielding made of lead bricks. The efficiency for the searched γ - γ coincidences was estimated through very accurate calibrations with a ^{102m}Rh source (that emits two γ rays having similar energies than the process searched for) and confirmed by Monte Carlo simulations. After 905 days of measurements, (35.5 ± 6.4) coincidence events were detected for the 539.5 keV and 590.8 keV γ quanta cascade following the $2\beta^-$ transition to the 0_1^+ excited state of ^{100}Ru (see Figure 3 (right)). As a result $T_{1/2} = [5.5^{+1.2}_{-0.8}(\text{stat.}) \pm 0.3(\text{syst.})] \times 10^{20}$ yr was obtained for the process searched for [24,25,27].

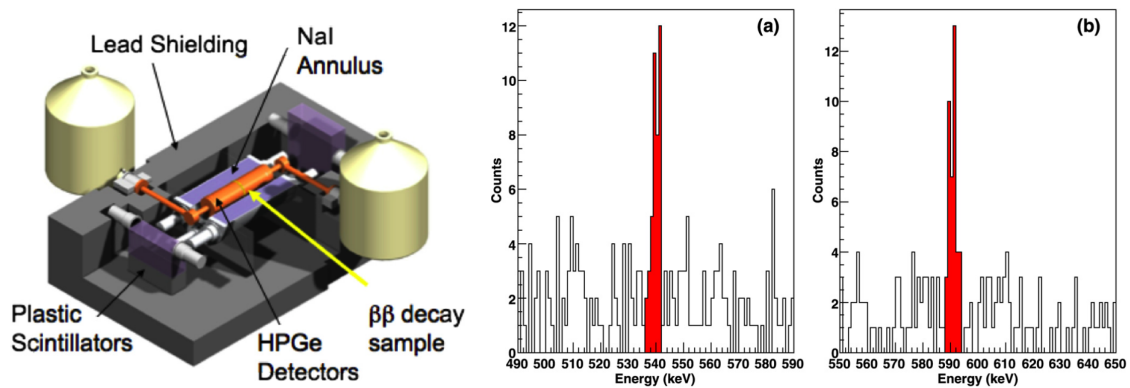


Figure 3. (left) Scheme of the experimental apparatus used in the TUNL-ITEP experiment (reprinted from Reference [31] with permission from American Physical Society). (right) Total collected events with the TUNL-ITEP apparatus over 905 days. (a) γ ray spectrum of events with energy around 540 keV in coincidence with the 590.8 keV transition in ^{100}Ru , and (b) γ ray spectrum of events with energy around 590 keV in coincidence with the 539.5 keV transition in ^{100}Ru (reprinted from Reference [27] with permission from Elsevier).

The NEMO collaboration released in 2007 new results on ^{100}Mo $2\beta^-$ decays to the excited levels of ^{100}Ru obtained with the NEMO-3 detector [26] at Modane Underground Laboratory (4800 m w.e. depth); a schematic view of the detector is shown in Figure 4 (left).

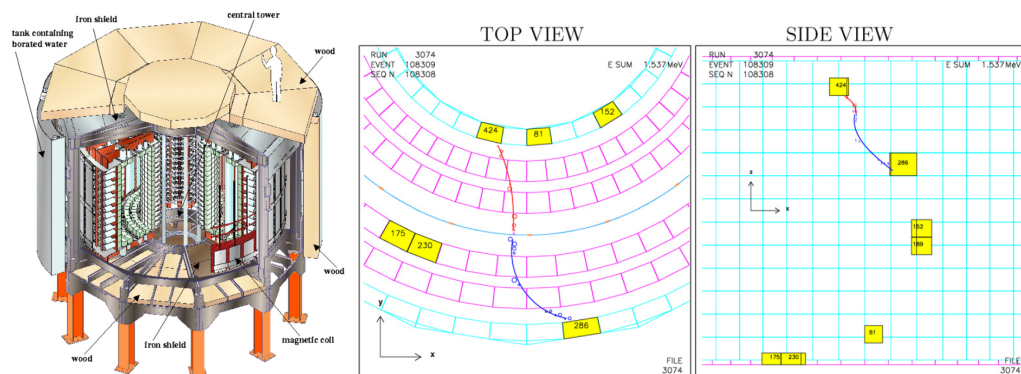


Figure 4. (left) Schematic view of the NEMO-3 detector. (right) A reconstructed event candidate for $2\beta^-$ decay of ^{100}Mo to the excited 0_1^+ state of ^{100}Ru . Two electrons of 424 and 286 keV energy, with a common origin in the source foil, hit fired isolated scintillators. The remaining fired scintillators compose three γ clusters, two are due to γ rays emitted in coincidence with the electrons, the third cluster is most probably due to the rescattering of one of these γ rays. Reprinted from Reference [26] with permission from Elsevier.

It was cylindrical in design ($\varnothing 6\text{ m} \times 4\text{ m}$) and composed of twenty equal sectors. There were three main components: a foil consisting of different sources of $\beta\beta$ decay isotopes, a tracker made of Geiger wire cells and a calorimeter made of scintillator blocks with PMT readout, surrounded by a solenoidal coil. The wire chamber was made of 6180 open octagonal drift cells operating in Geiger mode and able to provides a three-dimensional measurement of the charged particle tracks. The calorimeter, surrounding the wire chamber, was composed of 1940 plastic scintillator blocks coupled by light-guides to low-radioactivity PMTs. The apparatus could accommodate almost 10 kg of different $\beta\beta$ decay isotopes, comprising 6914 g of purified ^{100}Mo (average enrichment at 97.7%). The foils were placed inside the wire chamber in the central vertical plane of each sector. The whole detector was covered by inner and outer shields. Thanks to the tracking calorimeter, the NEMO-3 detector was able to identify the two electrons from $2\beta^-$ decay and the de-excitation photons from the excited state of the daughter nucleus. An example of reconstructed event candidate for $2\beta^-$ decay of ^{100}Mo to the

excited 0_1^+ state of ^{100}Ru is shown in Figure 4 (right). A large number of selection criteria based on energy, track, time and topology of the detected particles were applied in order to maximize the signal to background ratio and two methods of background estimation were used. After ~ 1 year of measurement, 37.5 signal events were obtained after cuts with an efficiency $(8.1 \pm 1.0) \times 10^{-4}$, which corresponds to $T_{1/2} = [5.7_{-0.9}^{+1.3}(\text{stat.}) \pm 0.8(\text{syst.})] \times 10^{20}$ yr [26].

In 2010, the ARMONIA experiment remeasured $\simeq 1$ kg of Mo enriched in ^{100}Mo to 99.5% already used in Reference [30] but with higher statistics and higher sensitivity [28]. After the first stage of the ARMONIA experiment, a purification procedure based on chemical transformation of metallic molybdenum to molybdenum oxide ($^{100}\text{MoO}_3$) was applied to the metallic ^{100}Mo powder. The measurements were performed at the Gran Sasso underground laboratory (LNGS) of the INFN in Italy (3600 m w.e. depth). The γ quanta with energies of 590.8 keV and 539.5 keV emitted in cascade in the de-excitation of the 0_1^+ excited level of ^{100}Ru were searched for using the GeMulti gamma spectrometer at STELLA facility of LNGS (see Reference [14] and Section 5.4). The set-up is composed of four low-background HP-Ge detectors ($\simeq 225$ cm³ each) allocated in one cryostat with a well in the center. The experimental set-up was enclosed in a lead and copper passive shielding and had a nitrogen ventilation system in order to avoid radon contamination. A schematic view of the $^{100}\text{MoO}_3$ source and the four HP-Ge detectors is shown in Figure 5 (left).

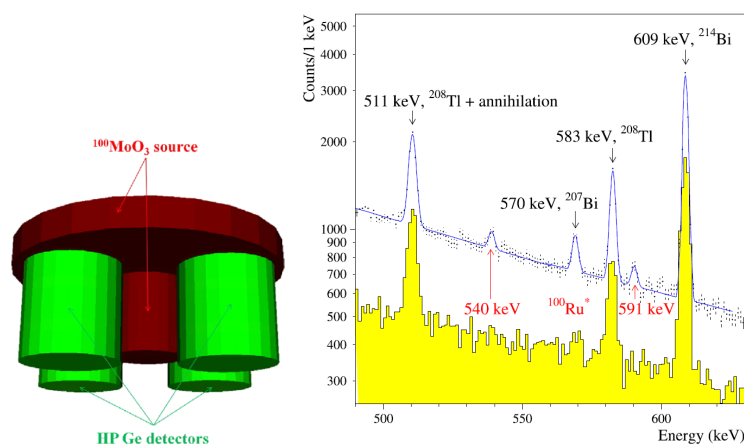


Figure 5. (left) Schematic view of the $^{100}\text{MoO}_3$ source and the four HP-Ge detectors used in the ARMONIA experiment (only the source and the detectors are shown). (right) Energy spectrum collected by the ARMONIA experiment with the $^{100}\text{MoO}_3$ sample (points with error bars) in the 490–630 keV energy interval together with its fit (continuous curve). The background spectrum (normalized to 18120 h) is also shown (filled histogram). Both peaks at 539.5 keV and 590.8 keV due to the $2\beta^-$ decay $^{100}\text{Mo} \rightarrow ^{100}\text{Ru}(0_1^+)$ are clearly visible in the $^{100}\text{MoO}_3$ spectrum. Reprinted from Reference [28] with permission from Elsevier.

The $^{100}\text{MoO}_3$ sample was measured for 18,120 h. The data acquisition system allowed to accumulate the energy spectra of the individual detectors and to take into account the coincidence between detectors during the data analysis as well. The background of the set-up was collected before and after the measurements with the sample, with consistent results. The 1-dimensional spectrum (sum of all 4 HP-Ge detectors) of the $^{100}\text{MoO}_3$ sample and of the background in the 490–630 keV energy interval is given in Figure 5 (right). Both peaks at 539.5 keV and 590.8 keV expected for $2\beta^-$ decay $^{100}\text{Mo} \rightarrow ^{100}\text{Ru}(0_1^+)$ are present in the spectrum collected with the $^{100}\text{MoO}_3$ sample and absent in the background spectrum. In particular, (319 ± 56) counts and (278 ± 53) counts were determined for the two peaks, respectively, fitting the $^{100}\text{MoO}_3$ spectrum. The efficiencies for the two γ lines were calculated with Montecarlo simulations, taking into account the angular correlation between the emitted γ quanta. Finally, joining the results from the two peaks, $T_{1/2} = (6.9_{-0.8}^{+1.0}(\text{stat.}) \pm 0.7(\text{syst.})) \times 10^{20}$ yr was obtained. This result was also confirmed by the analysis of the events with multiplicity 2 accumulated in coincidence mode. In particular, eight events

were detected in double coincidence for the 539.5 keV and 590.8 keV γ 's. They correspond to the half-life: $T_{1/2} = (6.8^{+3.7}_{-1.8}(\text{stat.})) \times 10^{20}$ yr [28].

In 2014, a new experiment [21] of the NEMO-3 collaboration was performed using a 2588 g sample of enriched ^{100}Mo metallic foil which was formerly inside the NEMO-3 detector (see above). In this case, the collaboration used a 600 cm³ low-background HP-Ge detector to measure the 2588 g sample of enriched ^{100}Mo metallic foil in a special delrin box which was placed around the detector end cap. Data were collected for 2288 h. The Ge spectrometer was composed of a p-type crystal. The cryostat, endcap, and the other mechanical parts were made of a very pure Al–Si alloy. The cryostat had a U-type geometry to shield the crystal from radioactive impurities in the dewar. The passive shielding was composed of three layers of Roman lead with a total thickness of ~ 12 cm and an external layer of ~ 20 cm of low radioactivity lead. A system for radon removal was present. Figure 6 shows the energy spectrum in the range of interest.

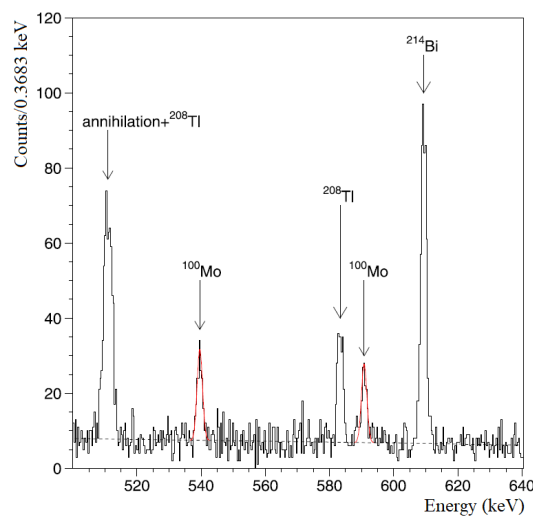


Figure 6. Energy spectrum in the range 500–640 keV obtained by the 2014 NEMO-3 collaboration experiment (reprinted from Reference [21] with permission from Elsevier). The dashed line is the estimated continuous background and colored (on-line) lines are the fitted peaks at 539.5 and 590.8 keV.

Both peaks at 539.5 keV and 590.8 keV are clearly visible, and the calculated area are (129 ± 14) counts and (110 ± 13) counts, respectively. From the combined analysis the half-life for the $2\beta^-$ decay of ^{100}Mo to the excited 0_1^+ state in ^{100}Ru was measured to be $T_{1/2} = [7.5 \pm 0.6(\text{stat.}) \pm 0.6(\text{syst.})] \times 10^{20}$ yr [21].

In conclusion, a summary of all the present positive results obtained in the search for $2\beta^-$ decay of ^{100}Mo to the first 0^+ excited state of ^{100}Ru is given in Table 2. The number of observed counts (N) and the signal-to-background ratio (S/B) are also reported. The average value was calculated in Reference [29], following the procedure recommended by the Particle Data Group [32].

Table 2. Present positive results on $T_{1/2}$ of the $2\beta^-$ decay of ^{100}Mo to the first 0^+ excited state of ^{100}Ru . N is the number of detected events or coincidences and S/B is the signal/background ratio.

$T_{1/2}$ (10^{20} yr)	N	S/B	Ref
$6.1^{+1.8}_{-1.1}$	133	1/7	[16]
$9.3^{+2.8}_{-1.7}(\text{stat.}) \pm 1.4(\text{syst.})$	153	1/4	[23]
$5.5^{+1.2}_{-0.8}(\text{stat.}) \pm 0.3(\text{syst.})$	35.5	8/1	[24,25,27]
$5.7^{+1.3}_{-0.9}(\text{stat.}) \pm 0.8(\text{syst.})$	37.5	3/1	[26]
$6.9^{+1.0}_{-0.8}(\text{stat.}) \pm 0.7(\text{syst.})$	597	1/10	[28]
$7.5 \pm 0.6(\text{stat.}) \pm 0.6(\text{syst.})$	239	2/1	[21]
Average value: $6.7^{+0.5}_{-0.4}$			[29]

4. Positive Results from $^{150}\text{Nd } 2\beta^-$ Decay to the 0_1^+ Excited Level

Another of the most interesting isotopes to study the $\beta\beta$ decay to excited levels is the ^{150}Nd . This nuclide is a very promising naturally occurring $\beta\beta$ isotope having a natural isotopic abundance of 5.638(28)% [18] and an high energy release: $Q_{\beta\beta} = 3371.38(20)$ keV [33]. The two neutrino decay mode to the ground state of ^{150}Sm has been observed in various experiments with a half-life in the range $(0.7 - 1.9) \times 10^{19}$ yr [34–36].

The $2\beta^-$ decay of ^{150}Nd to the 0_1^+ excited level (740.46 keV) of ^{150}Sm has been also investigated in several experiments reporting half-life in the range $(0.7 - 1.4) \times 10^{20}$ yr, as summarized in the following. The simplified $2\beta^-$ decay scheme of ^{150}Nd is reported in Figure 7. As can be seen, the 0_1^+ excited level of ^{150}Sm has an energy of 740.5 keV. From this level two gamma quanta of 406.5 keV and 334.0 keV, respectively, can be emitted in cascade to reach the ground level.

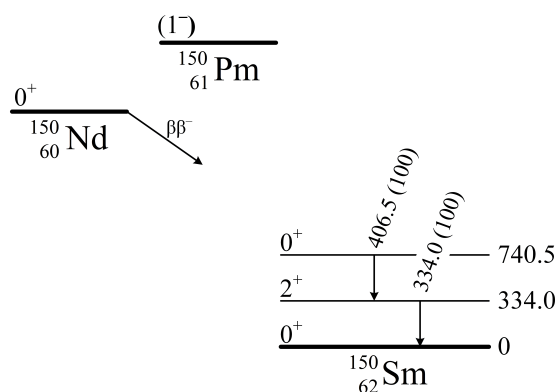


Figure 7. Simplified decay scheme of the $2\beta^-$ decay of ^{150}Nd to the 0_1^+ excited level of ^{150}Sm .

The first observation of this decay has been obtained in 2004 [17] with 3.046 kg of Nd_2O_3 in form of powder, measured for 11,320.5 h in a 400 cm^3 low background HP-Ge detector. The detector was surrounded by a low background passive shield and by a radon removal system. The signal is given by the presence of an excess of events at the energy values of the gamma's emitted in the ^{150}Sm de-excitation cascade. The energy spectrum measured in the experiment is reported in Figure 8; the two energy intervals of interest for the presence of the peaks searched for are reported.

In particular, the measured energy spectrum shows the presence of a peak at energy close to 334.0 keV, while the presence of the 406.5 keV peaks is somehow overlapped to a background peak ascribed to ^{211}Pb decay. After subtracting the estimated background, the excess for the 334.0 keV and 406.5 keV gamma lines correspond to (86 ± 28) and (100 ± 25) counts over a background of about 656.6 and 484.5 counts, respectively [17]. By summing the two peaks, the obtained half-life is: $T_{1/2} = [1.4_{-0.2}^{+0.4}(\text{stat.}) \pm 0.3(\text{syst.})] \times 10^{20}$ yr [17]. Some years later, the data analysis has been refined in Reference [37]. The full peak efficiencies for the gamma's searched for have been recalculated and smaller values for the excess counts—that is, (78.5 ± 28.4) and (99.0 ± 24.7) , respectively—have been obtained. The new half-life value was set to $T_{1/2} = [1.33_{-0.23}^{+0.36}(\text{stat.})_{-0.13}^{+0.27}(\text{syst.})] \times 10^{20}$ yr [37]. In the same paper other transitions to higher excited states were also searched for. No evidences have been found and lower limits on the half-lives of the $2\beta^-$ decay of ^{150}Nd to the 2_1^+ , 2_2^+ , 2_3^+ and 0_2^+ were set at level of about $(2 - 8) \times 10^{20}$ yr.

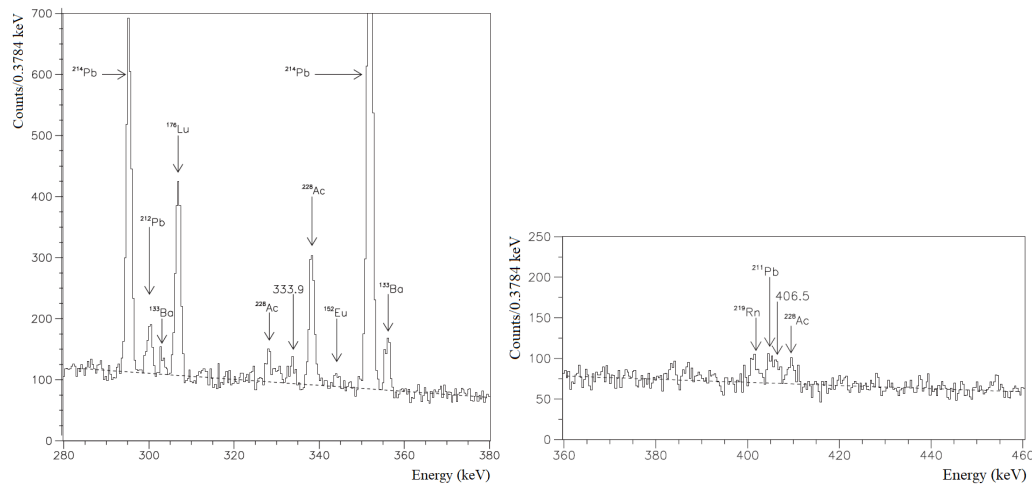


Figure 8. Energy spectrum collected in the HP-Ge experiment of Reference [17]. The two plots show the energy ranges of interest to search for the presence of the gamma’s related to the decay of the excited states of the daughter nucleus. Reprinted from Reference [37] with permission from American Physical Society.

A foil with 56.7 g of $^{150}\text{Nd}_2\text{O}_3$ enriched to ^{150}Nd at 91.0% has been used in the NEMO-3 experiment to measure the half-life of the $2\beta^-$ decay to excited level of the ^{150}Nd [38] (the set-up has already been described in Section 3). In the case of the double beta decay of ^{150}Nd to the 0_1^+ excited level of ^{150}Sm both electrons and gamma have been measured to reconstruct the full kinematics of the decay. A preliminary analysis has been performed in a PhD thesis and not published [38].

Another investigation on the $2\beta^-$ decay of ^{150}Nd to the 0_1^+ excited level of ^{150}Sm was also performed at the Kimballton Underground Research Facility [31] at a depth of 1450 m w.e. A compressed Nd_2O_3 powder of 50.00 g enriched to 93.60% in ^{150}Nd was placed, in a sandwich-like configuration, between the two HP-Ge detectors of the set-up already-discussed in Section 3, see Figure 3 (left). The strategy was to investigate the coincidences in the two HP-Ge detectors between the two γ quanta emitted in the de-excitation of the ^{150}Sm level. The experiment suffers of low detection efficiency; however, the possibility to identify the signal and the reached high signal-to-background ratio allowed to have enough sensitivity for the sought effect. The coincidence spectrum of both the HP-Ge detectors, corresponding to 642.8 days of measurement, is reported in Figure 9. After discarding the vetoed events and subtracting the background, (21.6 ± 6.4) events in coincidence were observed and the half-life of the decay has been established to $T_{1/2} = [1.07^{+0.45}_{-0.25}(\text{stat.}) \pm 0.07(\text{syst.})] \times 10^{20}$ yr [31].

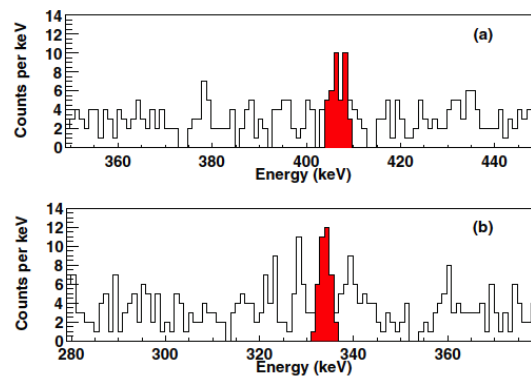


Figure 9. Coincidence plots collected in the experiment at Kimballton: (a) spectrum of events with energy around 406 keV in coincidence with a gamma of 334.0 keV; (b) spectrum of events with energy around 334 keV in coincidence with a gamma of 406.5 keV. Reprinted from Reference [31] with permission from American Physical Society.

At present an experiment to perform a further measurement of the $2\beta^-$ decay to excited states of ^{150}Nd is ongoing at the STELLA facility of LNGS [14], using Nd_2O_3 powder as source. This powder, used also in previous measurements [17,37], has preliminarily undergone chemical and physical purification procedures based on the precipitation of the material from a solution and on the liquid-liquid extraction method [39,40]. The powder was then pressed into 20 cylindrical tablets ($\varnothing 16.0 \times 56$ mm each), corresponding to a total mass of 2.381 kg. The tablets were placed in GeMulti gamma spectrometer (see Section 3 and Figure 5 (left)), where time and amplitude of events in each detector are recorded. The energy resolution of the four spectrometers has been estimated by standard gamma sources. During the data taking the energy scale and the resolution of the detectors have been monitored by considering few background peaks.

The approach pursued by the experiment is the measurement of the cumulative spectrum collected with the four HP-Ge detectors to point out the presence of the 334.0 keV and the 406.5 keV peaks ascribed to the gamma transitions from the ^{150}Sm 0_1^+ excited level. In addition, the coincidence spectrum has also been studied. In the decay searched for, in fact, one expects to observe the two de-excitation gammas in coincidence in two different HP-Ge detectors.

In particular, a dedicated correlation analysis of the two gamma lines in the energy spectrum acquired by the HPGe diodes has been performed. The presence of such correlated events is the signature of the sought decay. In the last analysis (previous data releases were reported in [41,42]) the data collected over 34,174 h have been considered [43]. The background spectrum obtained in 7862 h of measurement without inserting in GeMulti the Nd_2O_3 powder has also been considered for comparison. The cumulative energy spectra obtained in this experiment are reported in Figure 10. In particular, in the left and right plots one can see the excess of events observed at 334.0 keV and at 406.5 keV respectively. The estimated number of counts for these two peaks was (492 ± 110) and (203 ± 93) , respectively.

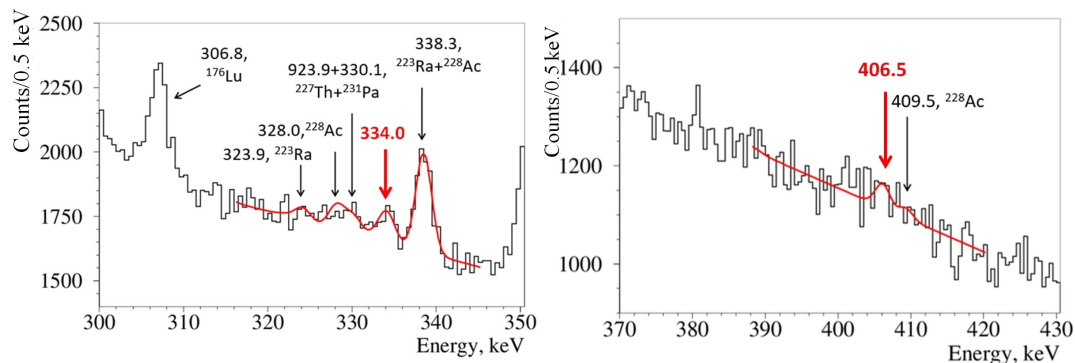


Figure 10. Spectra collected over 34,174 h by measuring Nd_2O_3 powder in the four HP-Ge detectors (GeMulti) at STELLA facility of LNGS. The two plots refer to the regions of interest to search for de-excitation gamma of the 0_1^+ level of ^{150}Sm [43].

The two expected peaks have also been observed in the two coincidence spectra (see Figure 11). In particular, the obtained number of coincidence events is: $[6.0_{-2.7}^{+3.3}(\text{stat.}) \pm 0.9(\text{syst.})]$. On the contrary, there is no evidence for peaks in the background coincidence spectrum, achieved by random coincidences when the energy of events in one of the detectors is taken as $375 \text{ keV} \pm 1.4 \times \text{FWHM}$, where no gamma is expected (see Figure 11 (bottom)). From a combined analysis of these measurements, a preliminary value for the half-life of the double beta decay of ^{150}Nd to the 0_1^+ excited level of ^{150}Sm has been set as: $[8.4_{-1.4}^{+2.2}(\text{stat.})_{-0.8}^{+4.4}(\text{syst.})] \times 10^{19} \text{ yr}$ [43].

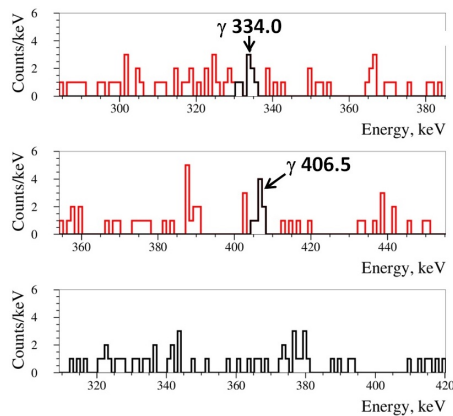


Figure 11. Coincidence spectra obtained in the experiment performed at STELLA facility of LNGS by using the four HP-Ge (GeMulti) detectors. In the top (middle) plot the spectrum of events with energy around 334 keV (406.5 keV) measured in coincidence with a 406.5 keV (334.0 keV) gamma in one HP-Ge detector is reported; the plot in the bottom represents a random coincidence background spectrum, see text and Reference [43].

Finally, the half-life measurements available so far for the double beta decay of ^{150}Nd to the 0_1^+ excited level of ^{150}Sm are summarized in Table 3. The number of observed counts (N) and the signal-to-background ratio (S/B) are also reported. The average value has been calculated following the procedure recommended by the Particle Data Group [32], and considering that the values of References [17,41,42] are preliminary and are not included in the average. Further more accurate measurements are foreseen by the experiment at LNGS, still running in order to increase the statistics and improve the sensitivity to the studied process.

Table 3. Half-life values of the $2\beta^-$ decay of ^{150}Nd to the 0_1^+ excited level of ^{150}Sm measured so far by different experiments. N is the number of detected events or coincidences and S/B is the signal/background ratio.

$T_{1/2}(10^{20})$ yr	N	S/B	Ref
$1.4^{+0.4}_{-0.2}(\text{stat.}) \pm 0.3(\text{syst.})$	186	1/8 – 1/5	[17]
$1.33^{+0.36}_{-0.23}(\text{stat.})^{+0.27}_{-0.13}(\text{syst.})$	177.5	1/9 – 1/5	[37]
$1.07^{+0.45}_{-0.25}(\text{stat.}) \pm 0.07(\text{syst.})$	21.6	1/1	[31]
$0.47^{+0.41}_{-0.19}(\text{stat.}) \pm 0.05(\text{syst.})$	5.7	3/1	[41]
$0.69^{+0.40}_{-0.19}(\text{stat.}) \pm 0.11(\text{syst.})$	6.1	3/1	[42]
$0.84^{+0.22}_{-0.14}(\text{stat.})^{+0.44}_{-0.08}(\text{syst.})$	6.0	3/1	[43]
Average value ^(a) : $1.18^{+0.23}_{-0.20}$			

^(a) Only the values of References [31,37,43] are considered. See text.

5. Limits Achieved in the Search for Other $\beta\beta$ Decay to Excited Levels

Many other results on different isotopes have been obtained in the search for double beta decay to excited levels of the daughter nuclei. In this section we only summarize the results of those isotopes more considered in the field. For the others isotopes we invite the reader to the bibliography [7,8,29,44–59].

The best present experimental results on the half-life, $T_{1/2}$, of the $2\beta^-$ decay (2ν and 0ν) to the excited levels of daughter nuclei for some of the isotopes most considered in the field are reported in Table 4. There, for simplicity only the transitions to the first 2^+ and 0^+ excited levels of daughter nucleus are considered. This is justified by the fact that higher excited levels correspond to lower decay rates and longer half-lives; moreover, other excited levels with larger multipolarity are strongly suppressed by the selection rules.

Table 4. Present best experimental results on the half-life, $T_{1/2}$, of the $2\beta^-$ decay (2ν and 0ν) to the excited levels of daughter nuclei (limits are at 90% C.L.) for some of the isotopes most considered in the field. Only the transitions to the first 2^+ and 0^+ excited levels of the daughter nucleus, if energetically allowed, are considered. See text.

Isotope	Process of Decay	Level of Daughter Nucleus (keV)	Nuclear De-Excitation γ 's (keV)	Experimental $T_{1/2}$ (yr)	
				$2\nu 2\beta^-$	$0\nu 2\beta^-$
^{48}Ca	$2\beta^-(0^+ \rightarrow 2_1^+)$	983.54	983.53	$\geq 1.8 \times 10^{20}$ [60]	$\geq 1.0 \times 10^{21}$ [61]
	$2\beta^-(0^+ \rightarrow 0_1^+)$	2997.22	983.53, 2013.66	$\geq 1.5 \times 10^{20}$ [60]	$\geq 1.5 \times 10^{20}$ [60]
^{76}Ge	$2\beta^-(0^+ \rightarrow 2_1^+)$	559.10	559.10	$\geq 7.7 \times 10^{23}$ [62]	$\geq 2.1 \times 10^{24}$ [62]
	$2\beta^-(0^+ \rightarrow 0_1^+)$	1122.28	559.10, 563.18	$\geq 7.5 \times 10^{23}$ [62]	$\geq 4.0 \times 10^{24}$ [62]
^{82}Se	$2\beta^-(0^+ \rightarrow 2_1^+)$	776.53	776.51	$\geq 1.3 \times 10^{22}$ [63]	$\geq 1.3 \times 10^{22}$ [63]
	$2\beta^-(0^+ \rightarrow 0_1^+)$	1487.70	776.51, 711.09	$\geq 3.4 \times 10^{22}$ [63]	$\geq 3.4 \times 10^{22}$ [63]
^{96}Zr	$2\beta^-(0^+ \rightarrow 2_1^+)$	778.24	778.22	$\geq 7.9 \times 10^{19}$ [64]	$\geq 9.1 \times 10^{20}$ [65]
	$2\beta^-(0^+ \rightarrow 0_1^+)$	1148.13	778.22, 369.80	$\geq 3.1 \times 10^{20}$ [66]	$\geq 3.1 \times 10^{20}$ [66]
^{100}Mo	$2\beta^-(0^+ \rightarrow 2_1^+)$	539.51	539.51	$\geq 2.5 \times 10^{21}$ [21]	$\geq 1.6 \times 10^{23}$ [26]
	$2\beta^-(0^+ \rightarrow 0_1^+)$	1130.32	539.51, 590.79	$(6.7^{+0.5}_{-0.4}) \times 10^{20}$ [29]	$\geq 8.9 \times 10^{22}$ [26]
^{104}Ru	$2\beta^-(0^+ \rightarrow 2_1^+)$	555.81	555.80	$\geq 6.6 \times 10^{20}$ [55]	$\geq 6.5 \times 10^{20}$ [55]
^{116}Cd	$2\beta^-(0^+ \rightarrow 2_1^+)$	1293.56	1293.56	$\geq 2.3 \times 10^{21}$ [67]	$\geq 7.1 \times 10^{22}$ [68]
	$2\beta^-(0^+ \rightarrow 0_1^+)$	1756.86	1293.56, 463.25	$\geq 2.0 \times 10^{21}$ [67]	$\geq 4.5 \times 10^{22}$ [68]
^{124}Sn	$2\beta^-(0^+ \rightarrow 2_1^+)$	602.73	602.73	$\geq 9.1 \times 10^{20}$ [69]	$\geq 9.1 \times 10^{20}$ [69]
	$2\beta^-(0^+ \rightarrow 0_1^+)$	1657.28	602.73, 1054.55	$\geq 1.2 \times 10^{21}$ [69]	$\geq 1.2 \times 10^{21}$ [69]
^{130}Te	$2\beta^-(0^+ \rightarrow 2_1^+)$	536.07	536.07	$\geq 1.9 \times 10^{21}$ [70]	$\geq 1.4 \times 10^{23}$ [71]
	$2\beta^-(0^+ \rightarrow 0_1^+)$	1793.52	536.07, 1257.5	$\geq 2.5 \times 10^{23}$ [72]	$\geq 1.4 \times 10^{24}$ [72]
^{134}Xe	$2\beta^-(0^+ \rightarrow 2_1^+)$	604.72	604.72	–	$\geq 2.6 \times 10^{22}$ [73]
^{136}Xe	$2\beta^-(0^+ \rightarrow 2_1^+)$	818.52	818.51	$\geq 4.6 \times 10^{23}$ [74]	$\geq 2.6 \times 10^{25}$ [74]
	$2\beta^-(0^+ \rightarrow 0_1^+)$	1578.97	818.51, 760.45	$\geq 8.3 \times 10^{23}$ [74]	$\geq 2.4 \times 10^{25}$ [74]
^{150}Nd	$2\beta^-(0^+ \rightarrow 2_1^+)$	333.96	333.96	$\geq 2.2 \times 10^{20}$ [37]	$\geq 2.4 \times 10^{21}$ [75]
	$2\beta^-(0^+ \rightarrow 0_1^+)$	740.46	333.96, 406.51	$(1.18^{+0.23}_{-0.20}) \times 10^{20}$ ^(a)	$\geq 2.4 \times 10^{20}$ [75]
^{154}Sm	$2\beta^-(0^+ \rightarrow 2_1^+)$	123.07	123.07	$\geq 6.0 \times 10^{18}$ [76]	$\geq 6.0 \times 10^{18}$ [76]
	$2\beta^-(0^+ \rightarrow 0_1^+)$	680.67	123.07, 557.58	$\geq 2.6 \times 10^{20}$ [76]	$\geq 2.6 \times 10^{20}$ [76]
^{170}Er	$2\beta^-(0^+ \rightarrow 2_1^+)$	84.25	84.25	$\geq 4.1 \times 10^{17}$ [77]	$\geq 4.1 \times 10^{17}$ [77]
^{176}Yb	$2\beta^-(0^+ \rightarrow 2_1^+)$	88.35	88.34	$\geq 4.5 \times 10^{16}$ [78]	$\geq 4.3 \times 10^{16}$ [78]
^{186}W	$2\beta^-(0^+ \rightarrow 2_1^+)$	137.16	137.16	$\geq 1.8 \times 10^{20}$ [54,79]	$\geq 1.1 \times 10^{21}$ [80]
^{192}Os	$2\beta^-(0^+ \rightarrow 2_1^+)$	316.51	316.51	$\geq 5.3 \times 10^{19}$ [81]	$\geq 5.3 \times 10^{19}$ [81]
^{198}Pt	$2\beta^-(0^+ \rightarrow 2_1^+)$	411.80	411.80	$\geq 3.5 \times 10^{18}$ [82]	$\geq 3.5 \times 10^{18}$ [82]

^(a) Value from Table 3.

Thus, considering that the transitions to the 2_1^+ level are more suppressed than those to the 0_1^+ level, and that the $\beta\beta$ decay to the 0_1^+ level provides a coincidences with two photons while only one photon is expected for the de-excitation of the 2_1^+ level, it appears very intriguing the study of the $\beta\beta(0^+ \rightarrow 0_1^+)$ decay. Actually, the only positive evidences are indeed obtained just for the $\beta\beta(0^+ \rightarrow 0_1^+)$ decay (see Sections 3 and 4).

The $2\beta^+$ decay to excited levels is allowed only for four nuclides and only involving the 2_1^+ level of the daughter nucleus. The best present experimental results on the half-life, $T_{1/2}$, of the $2\beta^+$ decay (2ν and 0ν) to the excited levels of daughter nuclei for all the isotopes where this transition is allowed are reported in Table 5. The reported measurements have been obtained by a BaF₂ crystal scintillator (mass of 3615 g) and two low background NaI(Tl) detectors for γ tagging [83] within the DAMA activities. Moreover, the measurements by the DAMA-INR Kyiv collaboration at LNGS, obtained with ¹⁰⁶CdWO₄ crystal scintillator in GeMulti [56] and in a closed (anti-)coincidence with two CdWO₄ [84] (see Section 5.3), are also reported.

Table 5. All the isotopes where the $2\beta^+$ decay (2ν and 0ν) to the excited levels of daughter nuclei is allowed. When available, the present best experimental result on $T_{1/2}$ (limits are at 90% C.L.) is reported. Only transitions to the first 2^+ excited level of the daughter nucleus are allowed. See text.

Isotope	Process of Decay	Level of Daughter Nucleus (keV)	Nuclear De-Excitation γ 's (keV)	Experimental $T_{1/2}$ (yr)	
				$2\nu 2\beta^+$	$0\nu 2\beta^+$
^{78}Kr	$2\beta^+(0^+ \rightarrow 2_1^+)$	613.73	613.73	–	–
^{106}Cd	$2\beta^+(0^+ \rightarrow 2_1^+)$	511.85	511.84	$\geq 2.5 \times 10^{21}$ [56]	$\geq 4.3 \times 10^{21}$ [84]
^{124}Xe	$2\beta^+(0^+ \rightarrow 2_1^+)$	602.73	602.73	–	–
^{130}Ba	$2\beta^+(0^+ \rightarrow 2_1^+)$	536.07	536.07	– ^(a)	$\geq 1.0 \times 10^{17}$ [83] ^(a)

^(a) A lower limit on the half-lives for all $\beta\beta$ decay modes of ^{130}Ba can be estimated by a geochemical experiment in Reference [47] as 1.5×10^{21} yr (90% C.L.) [45].

Let us note that a limit on the half-lives for all $\beta\beta$ decay modes of ^{130}Ba has been estimated by a geochemical experiment in Reference [47] as 1.5×10^{21} yr (90% C.L.) [45]. As shown, for the other nuclides there are no measurement yet.

Finally, Tables 6 and 7 show the present best experimental results on the half-life, $T_{1/2}$, of the $\varepsilon\beta^+$ and 2ε decay to the excited levels of daughter nuclei for some of the isotopes most considered in the field. As in Table 4, only the 2_1^+ and 0_1^+ excited levels, if energetically allowed, of the daughter nucleus are considered. In the following, for the $0\nu 2\varepsilon$ decay mode to the ground or to the excited levels of the daughter nucleus, we assume that the energy excess is taken away by bremsstrahlung γ quanta with energy $E_\gamma = Q - E_{b1} - E_{b2} - E_{exc}$, where E_{bi} are the binding energies of the captured electrons in the atomic shells of the daughter atom, and E_{exc} is the energy of the reached excited level. The experimental results available for resonant decay modes (see Section 2) are instead summarized in Table 8. Let us note that most of the limits reported in Tables 4–8 have been obtained within the DAMA activities and by the DAMA-INR Kyiv collaboration at LNGS (see also in the following, Sections 5.3 and 5.4).

Table 6. Some of the isotopes most considered in the field of the $\varepsilon\beta^+$ decay (2ν and 0ν) to the excited levels of daughter nuclei. When available, the present best experimental result on $T_{1/2}$ is also reported (limits are at 90% C.L.). Only the transitions to the first 2^+ and 0^+ excited levels of the daughter nucleus, if energetically allowed, are considered. See text.

Isotope	Process of Decay	Level of Daughter Nucleus (keV)	Nuclear De-Excitation γ 's (keV)	Experimental $T_{1/2}$ (yr)	
				$2\nu\varepsilon\beta^+$	$0\nu\varepsilon\beta^+$
^{78}Kr	$\varepsilon\beta^+(0^+ \rightarrow 2_1^+)$	613.73	613.73	–	–
	$\varepsilon\beta^+(0^+ \rightarrow 0_1^+)$	1498.60	613.73, 884.86	–	–
^{96}Ru	$\varepsilon\beta^+(0^+ \rightarrow 2_1^+)$	778.24	778.22	$\geq 2.3 \times 10^{20}$ [55]	$\geq 2.3 \times 10^{20}$ [55]
	$\varepsilon\beta^+(0^+ \rightarrow 0_1^+)$	1148.13	778.22, 369.80	$\geq 2.1 \times 10^{20}$ [55]	$\geq 2.1 \times 10^{20}$ [55]
^{106}Cd	$\varepsilon\beta^+(0^+ \rightarrow 2_1^+)$	511.85	511.84	$\geq 2.7 \times 10^{21}$ [84]	$\geq 9.7 \times 10^{21}$ [84]
	$\varepsilon\beta^+(0^+ \rightarrow 0_1^+)$	1133.76	511.84, 621.94	$\geq 1.1 \times 10^{21}$ [56]	$\geq 1.9 \times 10^{21}$ [56]
^{112}Sn	$\varepsilon\beta^+(0^+ \rightarrow 2_1^+)$	617.52	617.52	$\geq 7.0 \times 10^{20}$ [57]	$\geq 7.0 \times 10^{20}$ [57]
^{124}Xe	$\varepsilon\beta^+(0^+ \rightarrow 2_1^+)$	602.73	602.73	–	$\geq 4.2 \times 10^{17}$ ^(a) [85]
	$\varepsilon\beta^+(0^+ \rightarrow 0_1^+)$	1657.28	602.73, 1054.55	–	–
^{130}Ba	$\varepsilon\beta^+(0^+ \rightarrow 2_1^+)$	536.07	536.07	– ^(b)	$\geq 1.1 \times 10^{17}$ [83] ^(b)
^{136}Ce	$\varepsilon\beta^+(0^+ \rightarrow 2_1^+)$	818.52	818.51	$\geq 2.4 \times 10^{18}$ [86]	$\geq 2.3 \times 10^{18}$ [86]
^{144}Sm	$\varepsilon\beta^+(0^+ \rightarrow 2_1^+)$	696.56	696.51	$\geq 3.2 \times 10^{19}$ [76]	$\geq 3.2 \times 10^{19}$ [76]
^{156}Dy	$\varepsilon\beta^+(0^+ \rightarrow 2_1^+)$	88.97	89.0	$\geq 1.9 \times 10^{16}$ [87]	$\geq 1.9 \times 10^{16}$ [87]
^{162}Er	$\varepsilon\beta^+(0^+ \rightarrow 2_1^+)$	80.66	80.66	$\geq 3.8 \times 10^{17}$ [77]	$\geq 3.7 \times 10^{17}$ [77]
^{168}Yb	$\varepsilon\beta^+(0^+ \rightarrow 2_1^+)$	79.80	79.80	$\geq 2.8 \times 10^{17}$ [78]	$\geq 2.8 \times 10^{17}$ [78]
^{184}Os	$\varepsilon\beta^+(0^+ \rightarrow 2_1^+)$	111.22	111.22	$\geq 2.5 \times 10^{16}$ [81]	$\geq 2.4 \times 10^{16}$ [81]
^{190}Pt	$\varepsilon\beta^+(0^+ \rightarrow 2_1^+)$	186.72	186.72	$\geq 8.4 \times 10^{15}$ [82]	$\geq 8.4 \times 10^{15}$ [82]

^(a) The limit is at 68% C.L. and it is for the K-shell electron capture. ^(b) A lower limit on the half-lives for all $\beta\beta$ decay modes of ^{130}Ba can be estimated by a geochemical experiment in Reference [47] as 1.5×10^{21} yr (90% C.L.) [45].

Table 7. Some of the isotopes most considered in the field of the 2ε decay (2ν and 0ν) to the excited levels of daughter nuclei. When available, the present best experimental result on $T_{1/2}$ is also reported (limits are at 90% C.L.). Only the transitions to the first 2^+ and 0^+ excited levels of the daughter nucleus, if energetically allowed, are considered. See text.

Isotope	Process of Decay	Level of Daughter Nucleus (keV)	Nuclear De-Excitation γ 's (keV)	Experimental $T_{1/2}$ (yr)	
				$2\nu 2\varepsilon$	$0\nu 2\varepsilon$
⁷⁴ Se	$2\varepsilon(0^+ \rightarrow 2^+)$	595.85	595.85	$\geq 1.8 \times 10^{19}$ [88]	$\geq 1.6 \times 10^{19}$ (2K) [88]
⁷⁸ Kr	$2\varepsilon(0^+ \rightarrow 2^+)$	613.73	613.73	–	–
	$2\varepsilon(0^+ \rightarrow 0^+)$	1498.60	613.73, 884.86	$\geq 5.4 \times 10^{21}$ (2K) [49]	–
⁸⁴ Sr	$2\varepsilon(0^+ \rightarrow 2^+)$	881.61	881.61	$\geq 3.1 \times 10^{16}$ [89]	$\geq 2.6 \times 10^{16}$ [89]
⁹⁶ Ru	$2\varepsilon(0^+ \rightarrow 2^+)$	778.24	778.22	$\geq 2.6 \times 10^{20}$ [55]	$\geq 2.4 \times 10^{20}$ [55]
	$2\varepsilon(0^+ \rightarrow 0^+)$	1148.13	778.22, 369.80	$\geq 2.5 \times 10^{20}$ [55]	$\geq 2.3 \times 10^{20}$ [55]
¹⁰⁶ Cd	$2\varepsilon(0^+ \rightarrow 2^+)$	511.85	511.84	$\geq 9.9 \times 10^{20}$ [56]	$\geq 5.1 \times 10^{20}$ [90]
	$2\varepsilon(0^+ \rightarrow 0^+)$	1133.76	511.84, 621.94	$\geq 1.0 \times 10^{21}$ [56]	$\geq 1.1 \times 10^{21}$ [56]
¹¹² Sn	$2\varepsilon(0^+ \rightarrow 2^+)$	617.52	617.52	$\geq 1.2 \times 10^{21}$ [57]	$\geq 9.7 \times 10^{20}$ [57]
	$2\varepsilon(0^+ \rightarrow 0^+)$	1224.34	617.52, 606.82	$\geq 1.6 \times 10^{21}$ [57]	$\geq 1.3 \times 10^{21}$ [57]
¹²⁴ Xe	$2\varepsilon(0^+ \rightarrow 2^+)$	602.73	602.73	–	–
	$2\varepsilon(0^+ \rightarrow 0^+)$	1657.28	602.73, 1054.55	–	–
¹³⁰ Ba	$2\varepsilon(0^+ \rightarrow 2^+)$	536.07	536.07	– ^(a)	– ^(a)
	$2\varepsilon(0^+ \rightarrow 0^+)$	1793.52	536.07, 1257.50	– ^(a)	– ^(a)
¹³⁶ Ce	$2\varepsilon(0^+ \rightarrow 2^+)$	818.52	818.51	$\geq 2.9 \times 10^{18}$ [86]	$\geq 3.0 \times 10^{18}$ [86]
	$2\varepsilon(0^+ \rightarrow 0^+)$	1578.97	818.51, 760.45	$\geq 2.5 \times 10^{18}$ [86]	$\geq 2.2 \times 10^{18}$ [86]
¹⁴⁴ Sm	$2\varepsilon(0^+ \rightarrow 2^+)$	696.56	696.51	$\geq 1.6 \times 10^{19}$ (2K) [76]	$\geq 1.4 \times 10^{19}$ (2K) [76]
¹⁵⁶ Dy	$2\varepsilon(0^+ \rightarrow 2^+)$	88.97	88.97	$\geq 1.8 \times 10^{14}$ [87]	$\geq 1.5 \times 10^{14}$ [87]
	$2\varepsilon(0^+ \rightarrow 0^+)$	1049.49	88.97, 960.51	$\geq 7.1 \times 10^{16}$ [87]	$\geq 6.4 \times 10^{16}$ [87]
¹⁶² Er	$2\varepsilon(0^+ \rightarrow 2^+)$	80.66	80.66	$\geq 1.2 \times 10^{16}$ [77]	$\geq 6.2 \times 10^{17}$ (2K) [77]
	$2\varepsilon(0^+ \rightarrow 0^+)$	1400.26	80.66, 1319.60	$\geq 1.3 \times 10^{18}$ [77]	$\geq 1.3 \times 10^{18}$ (2K) [77]
¹⁶⁸ Yb	$2\varepsilon(0^+ \rightarrow 2^+)$	79.80	79.80	$\geq 2.3 \times 10^{15}$ [78]	$\geq 4.4 \times 10^{14}$ [78]
	$2\varepsilon(0^+ \rightarrow 0^+)$	1217.17	79.80, 1137.36	$\geq 1.5 \times 10^{18}$ [78]	$\geq 1.5 \times 10^{18}$ [78]
¹⁷⁴ Hf	$2\varepsilon(0^+ \rightarrow 2^+)$	76.47	76.47	$\geq 5.9 \times 10^{16}$ (2K) [91]	$\geq 7.1 \times 10^{17}$ (2K) [91]
¹⁸⁴ Os	$2\varepsilon(0^+ \rightarrow 2^+)$	111.22	111.22	$\geq 3.1 \times 10^{15}$ [81]	$\geq 3.3 \times 10^{17}$ (2K) [81]
	$2\varepsilon(0^+ \rightarrow 0^+)$	1002.49	111.22, 891.27	$\geq 3.8 \times 10^{17}$ [81]	$\geq 3.5 \times 10^{17}$ [81]
¹⁹⁰ Pt	$2\varepsilon(0^+ \rightarrow 2^+)$	186.72	186.72	$\geq 8.8 \times 10^{14}$ (2K) [82]	$\geq 6.9 \times 10^{14}$ [82]
	$2\varepsilon(0^+ \rightarrow 0^+)$	911.78	186.72, 725.07	$\geq 4.5 \times 10^{15}$ (2K) [82]	$\geq 3.6 \times 10^{15}$ [82]

^(a) A lower limit on the half-lives for all $\beta\beta$ decay modes of ¹³⁰Ba can be estimated by a geochemical experiment in Reference [47] as 1.5×10^{21} yr (90% C.L.) [45].

Table 8. Present best experimental results on $T_{1/2}$ of the resonant $0\nu 2\varepsilon$ decay (limits are at 90% C.L.) for some of the isotopes most considered in the field. See text.

Isotope	Process of Decay	Level of Daughter Nucleus (keV)		Experimental $T_{1/2}$ (yr)
⁷⁴ Se	Resonant $0\nu 2L$	1204.20	2^+	$\geq 1.1 \times 10^{19}$ [88]
⁷⁸ Kr	Resonant $0\nu 2K$	2838.49	(2^+)	$\geq 5.4 \times 10^{21}$ [49]
⁹⁶ Ru	Resonant $0\nu KL$	2700.21	2^+	$\geq 2.0 \times 10^{20}$ [55]
	Resonant $0\nu 2L$	2712.68		$\geq 3.6 \times 10^{20}$ [55]
¹⁰⁶ Cd	Resonant $0\nu 2K$	2717.59		$\geq 2.9 \times 10^{21}$ [84]
	Resonant $0\nu KL_1$	2741.0	4^+	$\geq 9.5 \times 10^{20}$ [90]
	Resonant $0\nu KL_3$	2748.2	$2, 3^-$	$\geq 1.4 \times 10^{21}$ [56]
¹¹² Sn	Resonant $0\nu 2K$	1870.68	4^+	$\geq 1.1 \times 10^{21}$ [57]
	Resonant $0\nu 2K$	1870.96	0^+	$\geq 1.3 \times 10^{21}$ [57]
¹²⁴ Xe	Resonant $0\nu 2K$	2808.66	2^+	–
	Resonant $0\nu KL$	2853.2		–
¹³⁰ Ba	Resonant $0\nu 2K$	2544.43		– ^(a)
	Resonant $0\nu 2L$	2608.43		– ^(a)
¹⁵² Gd	Resonant $0\nu KL$	g.s.	0^+	–
¹⁵⁶ Dy	Resonant $0\nu 2K$	1914.83	2^+	$\geq 1.1 \times 10^{16}$ [87]
	Resonant $0\nu KL_1$	1946.34	1^-	$\geq 1.0 \times 10^{18}$ [92]
	Resonant $0\nu KL_1$	1952.40	0^-	$\geq 2.2 \times 10^{17}$ [92]
	Resonant $0\nu 2L_1$	1988.5	0^+	$\geq 9.5 \times 10^{17}$ [92]
	Resonant $0\nu 2L_3$	2003.75	2^+	$\geq 6.7 \times 10^{16}$ [92]
¹⁵⁸ Dy	Resonant $0\nu 2L_1$	261.5	4^+	$\geq 3.2 \times 10^{16}$ [87]
¹⁶² Er	Resonant $0\nu KL_1$	1782.68	(2^+)	$\geq 5.0 \times 10^{17}$ [77]
¹⁶⁴ Er	Resonant $0\nu 2L$	g.s.	0^+	–
¹⁶⁸ Yb	Resonant $0\nu 2M_1$	1403.74	(2^-)	$\geq 1.9 \times 10^{18}$ [78]
¹⁸⁰ W	Resonant $0\nu 2K$	g.s.	(0^+)	$\geq 1.3 \times 10^{18}$ [54]
¹⁸⁴ Os	Resonant $0\nu 2K$	1322.15	(0^+)	$\geq 2.8 \times 10^{16}$ [81]
	Resonant $0\nu KL$	1386.30	2^+	$\geq 6.7 \times 10^{16}$ [81]
	Resonant $0\nu 2L$	1431.02	2^+	$\geq 8.2 \times 10^{16}$ [81]
¹⁹⁰ Pt	Resonant $0\nu(2M, MN, 2N)$	1382.4	($0, 1, 2^+$)	$\geq 2.9 \times 10^{16}$ [82]

^(a) A lower limit on the half-lives for all $\beta\beta$ decay modes of ¹³⁰Ba can be estimated by a geochemical experiment in Reference [47] as 1.5×10^{21} yr (90% C.L.) [45].

In the following, we illustrate the used techniques and their potentiality, taking as example some of the experiments in the field of $2\beta^-$, $2\beta^+$, $\epsilon\beta^+$, and 2ϵ decay to excited levels of daughter nuclei.

5.1. Examples of Experiments with Germanium Detectors as Active Source

The germanium detectors were one of the first kind of detectors ever used in the field of $\beta\beta$ decay; the first experimental study on $\beta\beta$ decay to the excited levels of the daughter nuclei was indeed reported by a germanium detector [12]. Since germanium contains the ^{76}Ge nuclide (natural isotopic abundance 7.8%) and isotopic enrichments are also possible and feasible, the detector coincides with the source itself. Thus, ^{76}Ge is one of the most investigated isotopes for the $\beta\beta$ decay ($Q_{\beta\beta} = 2039.061(7)$ keV [93]); it can decay to three excited levels of the daughter nucleus, ^{76}Se , with clear event signatures consisting of a $2\beta^-$ decay followed by the prompt emission of one or two γ quanta. The level scheme of such a decay is reported in Figure 12.

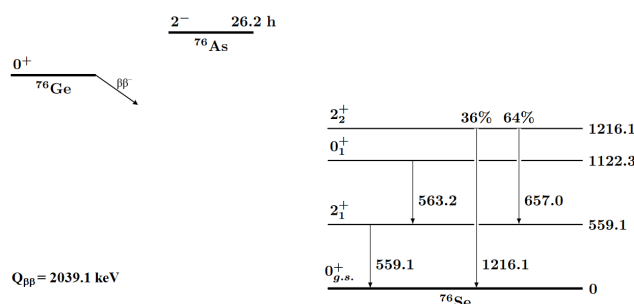


Figure 12. Scheme of $2\beta^-$ decay of ^{76}Ge to the ground state and to the first excited levels of ^{76}Se . The energies of the levels and the relative main branching ratios are taken from Reference [94].

Progress and efforts in the improvements of low-level of radioactivity measurements techniques has favoured the studies on double beta decay of ^{76}Ge isotope. This is the case, for example, of the half-life limits achieved for the $(2\nu + 0\nu)2\beta^-$ of ^{76}Ge to excited states of ^{76}Se deduced from the background screening of a passive shield using an HP-Ge detector in Reference [95]. Present results, indeed, have been profited of a long history of experimental technical improvements, of new deep underground laboratories and an increase of expertise in the sector.

The two most sensitive Ge-based experiments running nowadays are GERDA experiment and MAJORANA DEMONSTRATOR (MJD). Actually, both experiments have reached a sensitivity, for the half-life of the double beta decay to excited states of daughter nucleus, at the level of 10^{23-24} yr. In particular, the MJD has published the most stringent limits for all the $2\beta^-$ processes to excited levels of ^{76}Se , both for 2ν and 0ν emission, as reported in Table 4. Thus, in the following, such results will be briefly described.

The MJD experiment is located deep underground at Sanford Laboratory, and consists of two modules, each one composed of an array of HP-Ge detectors operated in vacuum and cooled down with two separate cryostats. The granularity of the set-up, common in the sector of rare events, allows a powerful discrimination of the event signature from background. The total number of HP-Ge detectors are 58 with a total mass of 44.1 kg, 28.7 kg of which is enriched to 88% to ^{76}Ge and the remaining 15.4 kg detectors have the natural isotopic abundance 7.8%. The shield of the detectors is composed of underground electroformed copper, commercially oxygen-free copper, and lead (see Figure 13 (left)). A radon removal system and a neutron shield are also present. The events have been selected in the region of interest (ROI) considering the expected γ quanta from the de-excitations of the energy levels of ^{76}Ge , as reported in Figure 13 (right). The data analysis is based on the double coincidence between the detector where $2\beta^-$ decay occurred releasing the energy of the two electrons and a second detector where the de-excitation γ rays are detected. To evaluate the detection efficiency, a Monte Carlo simulation has been developed. The complete analysis is described in Reference [62], and no effect has been observed. Therefore, the upper limits for the $T_{1/2}$ of $2\beta^-$ decay of ^{76}Ge to the excited states of

^{76}Se after an exposure of $41.9 \text{ kg} \times \text{yr}$ —corresponding to a $21.3 \text{ kg} \times \text{yr}$ for the isotopic exposure of ^{76}Ge —have been inferred. In particular, the half-life limits for the $(0^+ \rightarrow 2_1^+)$ and $(0^+ \rightarrow 0_1^+)$ transitions with/without neutrinos are reported in Table 4, while the half-life limits for the $(0^+ \rightarrow 2_2^+, 1216.1 \text{ keV})$ transitions are: $T_{1/2} \geq 1.3 \times 10^{24} \text{ yr}$ for the $2\nu 2\beta^-$ decay and $T_{1/2} \geq 9.7 \times 10^{23} \text{ yr}$ for the $0\nu 2\beta^-$ decay [62].

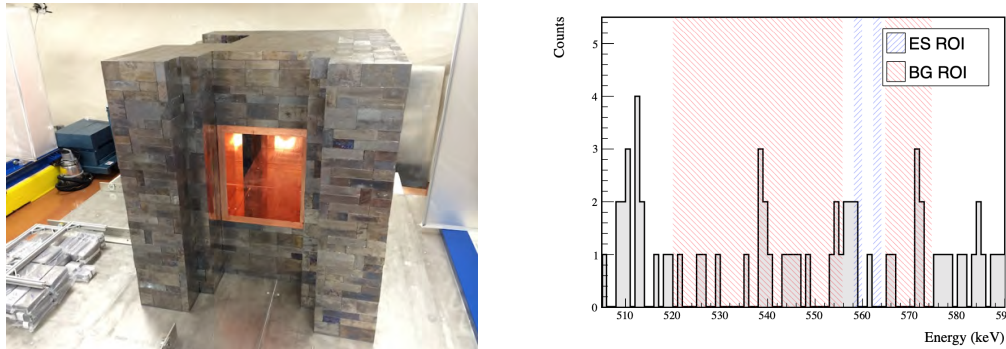


Figure 13. (left) Picture of the shield of MJD. It is possible to see the lead bricks and the inner copper shield (taken from Reference [96]). (right) MAJORANA measured energy spectrum after applying all the cuts (black histogram); the signal (ES=excited state) for the $2\nu 2\beta^-$ decay of ^{76}Ge to the 0_1^+ level of ^{76}Se is searched for in the energy region of the two expected gamma quanta: 559 keV and 563 keV. The background (BG) ROI where the background is evaluated is labelled too. Reprinted from Reference [97] under the terms of the Creative Commons Attribution 3.0 licence.

The GERmanium Detector Array (GERDA) experiment [98,99] is operating 37 detectors made from material enriched in ^{76}Ge and a total mass of 35.6 kg within a cryostat containing liquid argon (LAr) at LNGS. The experiment profits from the shielding of the LAr and its scintillation properties. The Ge detectors are installed in strings, and each detector-string is enclosed within a cylinder, made of $60 \mu\text{m}$ thick Cu foil, called “mini-shroud” for mitigating ^{42}K background due to the ^{42}Ar decay. Moreover, all the detector-strings are enclosed in a radon shroud made by a copper shield [98,99]. GERDA to date published limits for the $2\nu 2\beta^-$ decay to the excited $(2_1^+, 0_1^+, 2_2^+)$ levels of ^{76}Se at level of $(1.3 - 3.7) \times 10^{23} \text{ yr}$ [100]. For such analysis the GERDA exposure, in terms of ^{76}Ge isotopic exposure, is of $22.3 \text{ kg} \times \text{yr}$ [100].

Considering that the exposures of GERDA and MJD are rather similar, the better performance of MJD, in terms of sensitivity, with respect to GERDA can be attributed to: (i) MJD has higher detection efficiency in the ROI because of the LAr surrounding the GERDA HP-Ge detectors (not present in MJD); (ii) the dominant background in GERDA in the ROI for excited state decays is due to the decay of ^{42}K in its LAr shield (not present in MJD); (iii) MJD has better energy resolution due to the absence of cross-talk between detectors, which worsened GERDA’s resolution for multi-detector events [62].

5.2. Example of Bolometer Experiments as Active Source

The ^{130}Te is another among-the-most investigated isotopes for the $\beta\beta$ decay ($Q_{\beta\beta} = 2527.518(13) \text{ keV}$ [101–103]). The decay scheme of ^{130}Te to the ^{130}Xe is shown in Figure 14.

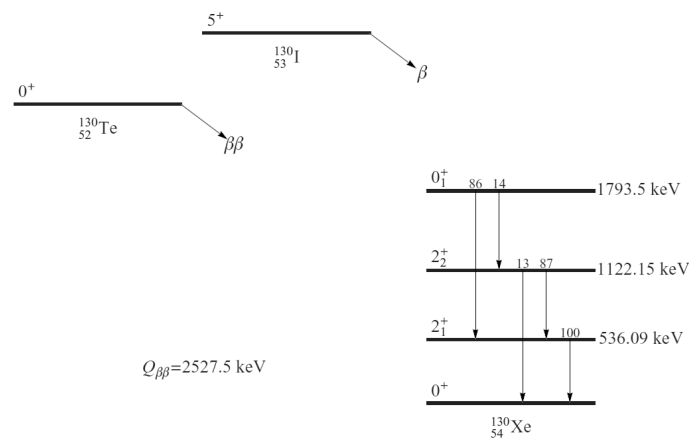


Figure 14. Scheme of $2\beta^-$ decay of ^{130}Te to the ground state and to the first excited levels of ^{130}Te (reprinted from Reference [72] under the terms of the Creative Commons Attribution 4.0 licence). The energies of the levels and the relative main branching ratios are taken from Reference [102].

To date, CUORE collaboration has reached the most competitive limits on the $2\beta^-$ decay of ^{130}Te in the excited state of ^{130}Xe . In particular, CUORE experiment, in its first stage named CUORE-0 experiment, has measured the most stringent limit on the decay to the 0_1^+ excited state in ^{130}Xe [72], improving its previous limit by the CUORE prototype experiment named CUORICINO and applying the same strategy and data analysis in both the studies [104]. However, CUORE-0 and CUORICINO have not investigated the $2\beta^-$ decay of ^{130}Te to the first (536.09 keV, 2_1^+) and second (1122.15 keV, 2_2^+) excited levels of ^{130}Xe . CUORE experiment is a cryogenic calorimeter using bolometers of TeO_2 crystals with natural abundance in ^{130}Te (34.2% [105]). Each crystal is a cube with 5 cm of edge, arranged in 19 towers; each tower is made by 52 TeO_2 crystal bolometers. CUORE-0 had been using only one tower of the CUORE experiment program (see Figure 15 (left)). The crystals of each tower are arranged in a copper frame into 13 floors, with each floor containing four crystals. The mass of each crystal is 750 g, each tower corresponds to 39 kg of TeO_2 and the isotopic mass of ^{130}Te is 10.8 kg. The operation temperature of each crystal is about 10 mK, monitored by a neutron transmutation doped thermistor [106] glued to the crystal surface. Different layers of shielding, as for example, an internal low-background Roman lead layer and an external anti-radon box, surround the cryostat and the crystals [107–109].

Considering the granularity of the multi-detectors set-up, several coincidence scenarios have been applied. The strategy, indeed, profits of a coincidence/anticoincidence logic between a first detector where the beta energy is released and a second or more detectors where the de-excited γ 's are fully absorbed (see for example Figure 15 (right)). The details of the analysis are reported in Reference [72]. Taking into account the data combination of CUORE-0 and CUORICINO, the achieved half-life limits for the case of $2\nu 2\beta^-$ and $0\nu 2\beta^-$ to the 0_1^+ excited level of ^{130}Xe are (at 90% C.L.) [72]: $T_{1/2}^{2\nu 2\beta^-} (0^+ \rightarrow 0_1^+) \geq 2.5 \times 10^{23}$ yr, and $T_{1/2}^{0\nu 2\beta^-} (0^+ \rightarrow 0_1^+) \geq 1.4 \times 10^{24}$ yr.

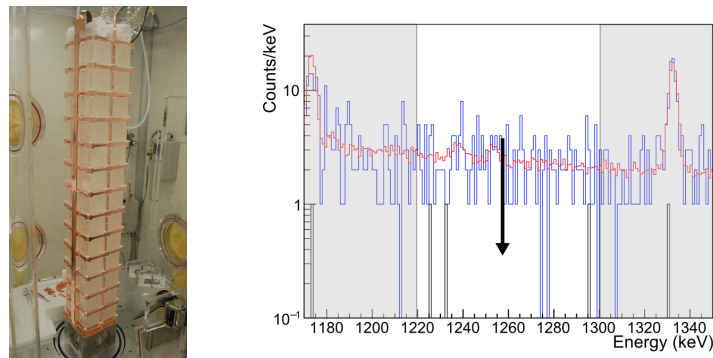


Figure 15. (left) The CUORE-0 tower (reprinted from Reference [107] with permission from IOP Publishing). (right) CUORE-0 spectra for the one of five signatures selected for the $2\nu 2\beta^-$ decay of ^{130}Te to the 0_1^+ level of ^{130}Xe . The blue histogram shows the data without any energy related cut; the reconstruction of the background model is shown in red; in black are data with energy cuts [72]. The black arrow points to the location of the expected peak. In particular this scenario considers three hits from 3 different detectors, in the same coincidence time window. One crystal must contain a signal with energy in the range $(734 \pm 5\sigma)$ keV; another one must have energy in the $(536 \pm 5\sigma)$ keV range. No requirement is imposed on the energy deposited in the third crystal. Reprinted from Reference [72] under the terms of the Creative Commons Attribution 4.0 licence.

To complete the picture about the investigation in the $2\beta^-$ decay of ^{130}Te to excited levels of ^{130}Xe , the following limits have also been reached: $T_{1/2}^{2\nu 2\beta^-} (0^+ \rightarrow 2_1^+) \geq 1.9 \times 10^{21}$ yr by exposing tellurium samples to a germanium detector [70], $T_{1/2}^{0\nu 2\beta^-} (0^+ \rightarrow 2_1^+) \geq 1.4 \times 10^{23}$ yr by using the calorimetric approach [71], and $T_{1/2}^{0\nu, 2\nu 2\beta^-} (0^+ \rightarrow 2_2^+) \geq 2.7 \times 10^{21}$ yr by exposing tellurium samples to two germanium detectors [110].

5.3. Examples of Experiments with Low-Background Scintillators

Low-background scintillators in double beta decay searches are used, in particular, within the DAMA activities and by the DAMA-INR Kyiv collaboration. In this Section a few of these activities will be summarized.

The AURORA experiment took data at LNGS for five years to investigate $2\beta^-$ decay processes in ^{116}Cd with 1.162 kg of enriched $^{116}\text{CdWO}_4$ scintillators [68]. Two cadmium tungstate crystals (580 g and 582 g) produced by means of the low-thermal-gradient Czochralski crystal growth technique from highly purified cadmium enriched in ^{116}Cd to 82% were used in the experiment. After several upgrades aiming at improving the detector background and energy resolution, the scintillators in the final stage were fixed inside polytetrafluoroethylene containers (see Figure 16) filled up with ultra-pure pseudocumene based liquid scintillator (LS). The passive shield and the plexiglas box for the radon removal system are shown in Figure 16 (left).

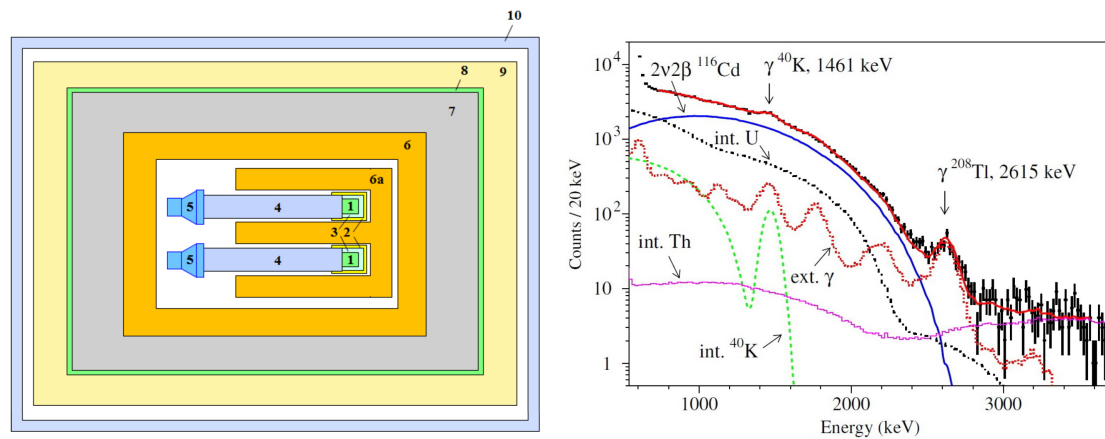


Figure 16. (left) Schematic view of the last AURORA set-up assembling. The two $^{116}\text{CdWO}_4$ crystal scintillators (1) are fixed in Teflon containers (2) filled up with liquid scintillator (3) and viewed through quartz light-guides (4) by photomultipliers (5). The passive shield consisted of high purity copper (6), additional high purity copper shield (6a), low radioactive lead (7), cadmium (8), polyethylene/paraffin (9), and plexiglas box for the radon removal system (10) [68]. (right) The energy spectrum of $\gamma(\beta)$ events accumulated over 26831 h with the $^{116}\text{CdWO}_4$ detectors together with the main components of the background model and the $2\nu 2\beta^-$ decay contribution (blue curve) [68]. Figures reprinted from Reference [68] with permission from American Physical Society.

There is a clear signature of the ^{116}Cd $2\nu 2\beta^-$ decay distribution in the energy spectrum of $\gamma(\beta)$ events selected by using the pulse-shape, time-amplitude and front-edge analyzes of the data accumulated over 26831 h (blue curve in Figure 16 (right)). The half-life relatively to $2\nu 2\beta^-$ decay to the ground state has precisely been measured as: $T_{1/2}^{2\nu 2\beta^-} = (2.63_{-0.12}^{+0.11}) \times 10^{19}$ yr. Stringent limits for $2\beta^-$ decay transitions to excited levels of ^{116}Sn (see Figure 17 (left)) have also been obtained [68], and some of them are reported in Table 4.

Another isotope of cadmium, ^{106}Cd , has been studied in an experiment, still running at LNGS, in the DAMA/CRYST set-up. In particular, a $^{106}\text{CdWO}_4$ crystal scintillator was the used detector [84]. The scheme of the experimental set-up is shown in Figure 18 (top). Two CdWO_4 crystal scintillators include a cylindrical cut-out to house the $^{106}\text{CdWO}_4$ crystal. The detector system was surrounded by four high purity copper bricks, low radioactive copper and lead, cadmium, and polyethylene in order to reduce the external background. Figure 18 (bottom), shows the energy spectrum of the $\gamma(\beta)$ events accumulated for 26033 h by the $^{106}\text{CdWO}_4$ scintillation detector in anti-coincidence with the CdWO_4 counters together with the background model [84]. The excluded distribution of the $0\nu 2\varepsilon$ decay of ^{106}Cd to the ground state of ^{106}Pd is also shown [84]. This experiment allowed to set new improved limits on various channels of ^{106}Cd double beta decay at the level of 10^{20} – 10^{22} yr (see Figure 17, right) [84]. In particular, for the channel $2\nu\varepsilon\beta^+$ to the ground state the half-life was estimated as $T_{1/2} \geq 2.1 \times 10^{21}$ yr [84]. The sensitivity is within the region of the theoretical predictions for the decay probability that are in the range of $T_{1/2} \approx (10^{21}$ – $10^{22})$ yr [84]. Some of these limits for decay channels to excited levels of ^{106}Pd —obtained by the running experiments and in their previous stages—are also reported in Tables 5–8.

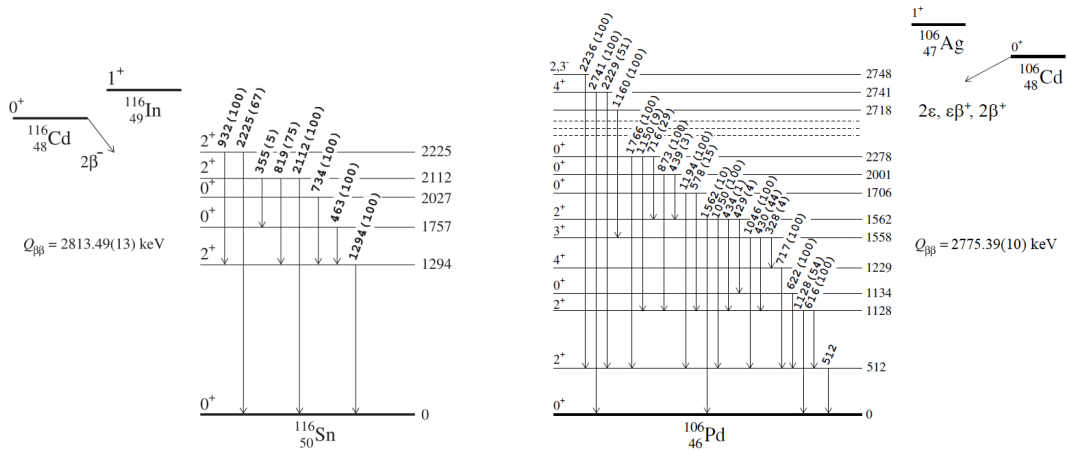


Figure 17. Simplified decay schemes of ^{116}Cd (left) and of ^{106}Cd (right). The energies of the excited levels and the emitted γ quanta are in keV; the relative intensities of γ quanta are given in parentheses. Their values are taken from References [68,84].

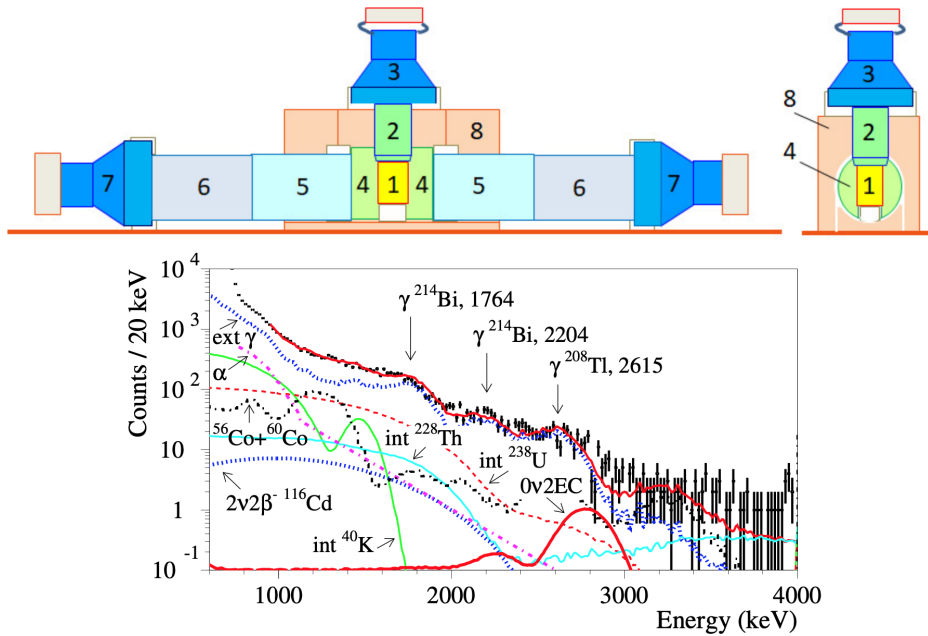


Figure 18. (top) Schematic of the experimental set-up with the $^{106}\text{CdWO}_4$ crystal scintillation detector (1), viewed through PbWO_4 light-guide (2) by PMT (3). Two CdWO_4 crystal scintillators (4) are viewed through light-guides glued from quartz (5) and polystyrene (6) by PMTs (7). The detector system was shielded by copper, lead, cadmium, and polyethylene (not shown). Only part of the copper details (8) is shown [84]. (bottom) Energy spectrum of the $\gamma(\beta)$ events accumulated for 26.033 h by the $^{106}\text{CdWO}_4$ scintillation detector in anti-coincidence with the CdWO_4 counters together with the background model (red line). The excluded distribution of the $0\nu 2\varepsilon$ decay of ^{106}Cd to the ground state of ^{106}Pd with the half-life $T_{1/2} = 6.8 \times 10^{20}$ yr is shown by red solid line [84]. Figures reprinted from Reference [84] under the terms of the Creative Commons Attribution license.

The next stage of experiment is running at LNGS in the DAMA/R&D set-up with an improved sensitivity to all of the decay channels, thanks to the reduction of the background approximately by a factor 3–5 due to ultra-radiopure PMTs, longer quartz light-guides for the CdWO_4 counters, and a more powerful passive shield of the detector system. The energy resolution of the $^{106}\text{CdWO}_4$ detector was also improved. As a result, the sensitivity to the $2\nu\varepsilon\beta^+$ decay of ^{106}Cd to the ground state is expected to be high enough to detect the process with the half-life at level of $\approx (0.5 - 1) \times 10^{22}$ yr over

five yr of measurements. Consequently, further improvements in the sensitivities to the transitions to the excited levels are also expected.

5.4. Some Other Experiments Exploiting the Passive Source Approach

The passive source approach has been exploited for some of the above-mentioned experiments. In this Section we briefly summarize the measurements carried out by the HP-Ge γ spectrometers at the STELLA facility of LNGS [14] by the DAMA-INR Kyiv collaboration (see also Sections 3 and 4). These detectors are mainly used for material screening needed for the experiments installed in the underground laboratories and the high level of their performance as ultra-low-level detector systems allows for detecting extremely low radioactivity levels in materials (typically down to the $\mu\text{Bq kg}^{-1}$ level). Some HP-Ge are used to search for various rare nuclear processes, which are accompanied by emission of gamma quanta and therefore also for double beta decays to excited states.

The experiments were carried out by using:

- the ultra-low background HP-Ge γ spectrometer GeCris (465 cm³, 120% relative efficiency with respect to a 3" \times 3" sodium iodine detector [14]). The detector is shielded with low radioactivity lead (\sim 25 cm), copper (\sim 5 cm), and, in the inner-most part, with archaeological Roman lead (\sim 2.5 cm). The set-up is placed in an air-tight poly-methyl-methacrylate box and flushed with high purity nitrogen gas to exclude the environmental radon. The purified samples were enclosed in a cylindrical polystyrene box on the HP-Ge detector end cap.
- the GeMulti set-up (made of four HP-Ge detectors inside the same cryostat; \simeq 225 cm³ each one). The detectors are surrounded by a passive shield made of low radioactivity copper (\simeq 5 cm) and low radioactivity lead (\simeq 25 cm). The set-up is continuously flushed with high purity nitrogen to remove residual radon.
- the ultra-low background HP-Ge detector GeBer (244 cm³). The detector is located inside a passive shield made of low radioactivity lead (\approx 20 cm), copper (\approx 10 cm) and borated polyethylene (\approx 10 cm). To remove radon, the set-up is continuously flushed by highly pure nitrogen.

The typical energy resolution of the detectors is 2.0 keV at the 1332.5 keV γ line of ⁶⁰Co. Other HP-Ge detectors are also used for radio-purity measurements [14]. The detection efficiencies of the processes searched for were Monte-Carlo simulated by using the EGSnrc [111] package and the GEANT4 package [112–114], with initial kinematics given by the DECAY0 event generator [115,116].

In particular, the measurements on ¹⁰⁰Mo and ¹⁵⁰Nd in GeMulti have already been discussed in Section 3 and 4, respectively. Campaigns of measurements were performed on a quite large number of elements containing isotopes candidates for $\beta\beta$ decay: samarium (¹⁴⁴Sm, ¹⁵⁴Sm) [76], ytterbium (¹⁶⁸Yb, ¹⁷⁶Yb) [78], erbium (¹⁶²Er, ¹⁷⁰Er) [77], cerium (¹³⁶Ce) [86,117,118], ruthenium (⁹⁶Ru, ¹⁰⁴Ru) [55,119], osmium (¹⁸⁴Os, ¹⁹²Os) [81], platinum (¹⁹⁰Pt, ¹⁹⁸Pt) [82], dysprosium (¹⁵⁶Dy, ¹⁵⁸Dy) [87], cadmium (¹⁰⁶Cd) [120], and tin (¹¹²Sn, ¹²⁴Sn) [121].

Some of these measurements are part of a program to explore the possibility to purify lanthanide elements and, using the purified samples, also to study their $\beta\beta$ processes in low-scale experiments [41,77,78,118]. The interest in purification is mainly related to ¹⁵⁰Nd, ¹⁶⁰Gd, and also rare-earth nuclides, which are among the most promising candidates for $0\nu\beta\beta$ decay searches. For samarium, ytterbium, erbium and dysprosium, the material contamination has been investigated by Inductively Coupled Plasma-Mass Spectrometry (ICP-MS). To reduce the observed radioactive contamination for samarium, ytterbium, erbium and cerium, purification of the material was performed using a combination of the sedimentation (precipitation) and liquid-liquid extraction [39] methods. The liquid-liquid extraction method has been proved to be the most effective technique for the purification of lanthanides from uranium and thorium traces [39,77,118].

Thanks to the procedures for purification of the used samples, to the high-purity and low-background HPGe detectors and to the underground facility, high sensitivities to the double beta decays to excited states have been reached; namely the best limits span from 10¹⁶ to 10²¹ yr, as reported in Tables 4–8.

6. Perspectives And Conclusions

The current interest and status of the experimental searches for $\beta\beta$ decay to the excited states of daughter nuclei have been outlined. In particular, several results have been obtained as a by-product of experiments whose main goal was the investigation of the $\beta\beta$ decay to the ground state. Further results profit of a wide variety of experimental set-ups with different sizes, even using materials enriched in the isotopes candidates for $\beta\beta$ decay. The improvements in low-background techniques, the chemical/physical purification of the used materials, and the possibility to locate the experiments in suitable underground sites allow for further background suppression. The large variety of techniques and experimental set-ups leads to perspectives in further improvements of the reachable sensitivities. Thus, in addition to the $\beta\beta$ decay to the 0_1^+ excited levels already-observed for the ^{100}Mo and ^{150}Nd cases, we could expect in future to have enough sensitivity for the detection of $\beta\beta$ decay to the 0_1^+ excited levels in other isotopes, as for example ^{96}Zr . Moreover, in the theoretical predictions reported in the framework of QRPA and pnQRPA nuclear models [122], $T_{1/2}$ values in the range 10^{21} – 10^{23} yr are reported for several nuclides both for $\beta\beta$ decay to the 0_1^+ and even 2_1^+ excited levels. All this gives the possibility to detect in near-future experiments even the 2_1^+ transitions, which allow the $\beta\beta$ field to access new information.

As it is well known, large efforts are planned in the future in the whole $\beta\beta$ decay field. For example, new results are foreseen by the CUORE experiment (using all its towers) at LNGS improving its half-life sensitivities [123], while – in the future – the two germanium collaborations (see Section 5.1) plan to join their efforts in the new LEGEND project, aiming at improving the sensitivity to the $2\beta^-$ decay in ^{76}Ge . Among the other existing efforts, the DAMA-INR Kiev collaboration is working in the purification of lanthanides aiming at improving the sensitivity in the passive source approach, and at growing crystals containing $\beta\beta$ candidate isotopes to be used as scintillators in *source=detector* approach.

All similar activities, when suitably supported, will also allow the investigation of the $\beta\beta$ decay to the excited states of daughter nuclei with significantly improved sensitivity, and thus increasing our knowledge in the $\beta\beta$ nuclear matrix elements and in the dynamics of the process.

Author Contributions: All the authors of this paper have been significantly contributing to the presented review of experimental results. All authors have read and agreed to the published version of the manuscript.

Funding: This research received no external funding.

Acknowledgments: It is a pleasure to thank all our collaborators in the searches on related fields.

Conflicts of Interest: The authors declare no conflict of interest.

References

1. Goepfert-Mayer, M. Double Beta-Disintegration. *Phys. Rev.* **1935**, *48*, 512. [[CrossRef](#)]
2. Furry, W.H. On Transition Probabilities in Double Beta-Disintegration. *Phys. Rev.* **1939**, *56*, 1184. [[CrossRef](#)]
3. Hirsch, M.; Muto, K.; Oda, T.; Klapdor-Kleingrothaus, H.V. Nuclear structure calculation of $\beta^+\beta^+$, β^+/EC and EC/EC decay matrix elements. *Z. Phys. A* **1994**, *347*, 151–160. [[CrossRef](#)]
4. Winter, R.G. Double K Capture and Single K Capture with Positron Emission. *Phys. Rev.* **1955**, *100*, 142–144. [[CrossRef](#)]
5. Voloshin, M.B.; Mitselmakher, G.V.; Eramzhyan, R.A. Conversion of an atomic electron into a positron and double β^+ decay. *JETP Lett.* **1982**, *35*, 656–659.
6. Bernabeu, J.; De Rujula, A.; Jarlskog, C. Neutrinoless double electron capture as a tool to measure the electron neutrino mass. *Nucl. Phys. B* **1983**, *223*, 15–28. [[CrossRef](#)]
7. Blaum, K.; Eliseev, S.; Danevich, F.A.; Tretyak, V.I.; Kovalenko, S.; Krivoruchenko, M.I.; Novikov, Y.N.; Suhonen, J. Neutrinoless Double-Electron Capture. *arXiv* **2020**, arXiv:2007.14908.
8. Krivoruchenko, M.I.; Simkovic, F.; Frekers, D.; Faessler, A. Resonance enhancement of neutrinoless double electron capture. *Nucl. Phys. A* **2011**, *859*, 140. [[CrossRef](#)]
9. Georgi, H.M.; Glashow, S.L.; Nussinov, S. Unconventional model of neutrino masses. *Nucl. Phys. B* **1981**, *193*, 297–316. [[CrossRef](#)]

10. Eliseev, S.A.; Novikov, Y.N.; Blaum, K. Search for resonant enhancement of neutrinoless double-electron capture by high-precision Penning-trap mass spectrometry. *J. Phys. G* **2012**, *39*, 124003. [[CrossRef](#)]
11. Belli, P. Special Issue: Low Background Techniques. *Int. J. Mod. Phys. A* **2017**, *32*. [[CrossRef](#)]
12. Fiorini, E. *Neutrino '77-Proceed. of the Intern. Conf. on Neutrino Physics and Neutrino Astrophysics, Baksan Valley, 18–24 June, 1977*; Nauka: Moscow, Russia, 1978; Volume 2, pp. 315–320.
13. Bellotti, E.; Fiorini, E.; Liguori, C.; Pullia, A.; Sarracino, A.; Zanotti, L. An experimental investigation on lepton number conservation in double-beta processes. *Lett. Nuovo Cim.* **1982**, *33*, 273. [[CrossRef](#)]
14. Laubenstein, M. Screening of materials with high purity germanium detectors at the Laboratori Nazionali del Gran Sasso. *Int. J. Mod. Phys. A* **2017**, *32*, 1743002. [[CrossRef](#)]
15. Barabash, A.S. A possibility for experimentally observing two-neutrino double beta decay. *JETP Lett.* **1990**, *51*, 207–209.
16. Barabash, A.S.; Avignone, F.T.; Collar, J.I.; Guerard, C.K.; Arthur, R.J.; Brodzinski, R.L.; Miley, H.S.; Reeves, J.H.; Meier, J.R.; Ruddick, K.; et al. Two neutrino double-beta decay of ^{100}Mo to the first excited 0^+ state in ^{100}Ru . *Phys. Lett. B* **1995**, *345*, 408. [[CrossRef](#)]
17. Barabash, A.S.; Hubert, F.; Hubert, P.; Umatov, V.I. Double-beta decay of ^{150}Nd to the first 0_1^+ excited state of $^{150}\text{Sm}^*$. *Phys. Atom. Nucl.* **2004**, *67*, 1216–1219. [[CrossRef](#)]
18. Meija, J.; Coplen, T.B.; Berglund, M.; Brand, W.A.; De Bièvre, P.; Gröning, M.; Holden, N.E.; Irrgeher, J.; Loss, R.D.; Walczyk, T.; et al. Isotopic compositions of the elements 2013 (IUPAC Technical Report). *Pure Appl. Chem.* **2016**, *88*, 293. [[CrossRef](#)]
19. Wang, M.; Audi, G.; Kondev, F.G.; Huang, W.J.; Naimi, S.; Xing, X. The Ame2016 atomic mass evaluation. *Chin. Phys. C* **2017**, *41*, 030003. [[CrossRef](#)]
20. Armengaud, E.; Augier, C.; Zolotarova, A.S. Precise measurement of $2\nu\beta\beta$ decay of ^{100}Mo with the CUPID-Mo detection technology. *Eur. Phys. J. C* **2020**, *80*, 674. [[CrossRef](#)]
21. Arnold, R.; Augier, C.; Barabash, A.S.; Basharina-Freshville, A.; Blondel, S.; Blot, S.; Bongrand, M.; Brudanin, V.; Busto, J.; Caffrey, A.J.; et al. Investigation of double beta decay of ^{100}Mo to excited states of ^{100}Ru . *Nucl. Phys. A* **2014**, *925*, 25–36. [[CrossRef](#)]
22. Singh, B. Nuclear Data Sheets for $A = 100$. *Nucl. Data Sheets* **2008**, *109*, 297. [[CrossRef](#)]
23. Barabash, A.S.; Gurriaran, R.; Hubert, F.; Hubert, P.; Umatov, V.I. $2\nu\beta\beta$ decay of ^{100}Mo to the first 0^+ excited state in ^{100}Ru . *Phys. At. Nucl.* **1999**, *62*, 2039–2043.
24. De Braeckeleer, L.; Hornish, M.; Barabash, A.; Umatov, V. Measurement of the $\beta\beta$ -Decay Rate of ^{100}Mo to the First Excited 0^+ State of ^{100}Ru . *Phys. Rev. Lett.* **2001**, *86*, 3510–3513. [[CrossRef](#)]
25. Hornish, M.J.; De Braeckeleer, L.; Barabash, A.S.; Umatov, V.I. Double β decay of ^{100}Mo to excited final states. *Phys. Rev. C* **2006**, *74*, 044314. [[CrossRef](#)]
26. Arnold, R.; Augier, C.; Baker, J.; Barabash, A.S.; Bongrand, M.; Broudin, G.; Brudanin, V.; Caffrey, A.J.; Egorov, V.; Etienvre, A.I.; et al. Measurement of double beta decay of ^{100}Mo to excited states in the NEMO 3 experiment. *Nucl. Phys. A* **2007**, *781*, 209–226. [[CrossRef](#)]
27. Kidd, M.F.; Esterline, J.H.; Tornow, W.; Barabash, A.S.; Umatov, V.I. New results for double-beta decay of ^{100}Mo to excited final states of ^{100}Ru using the TUNL-ITEP apparatus. *Nucl. Phys. A* **2009**, *821*, 251–261. [[CrossRef](#)]
28. Belli, P.; Bernabei, R.; Boiko, R.S.; Cappella, F.; Cerulli, R.; Danevich, F.A.; d'Angelo, S.; Incicchitti, A.; Kobaychev, V.V.; Kropivnyansky, B.N.; et al. New observation of $2\beta 2\nu$ decay of ^{100}Mo to the 0_1^+ level of ^{100}Ru in the ARMONIA experiment. *Nucl. Phys. A* **2010**, *846*, 143–156. [[CrossRef](#)]
29. Barabash, A.S. Average and recommended half-life values for two-neutrino double beta decay. *Nucl. Phys. A* **2015**, *935*, 52. [[CrossRef](#)]
30. Blum, D.; Busto, J.; Campagne, J.E.; Dassié, D.; Hubert, F.; Hubert, P.; Isaac, M.C.; Izac, C.; Jullian, S.; Kouts, B.N.; et al. Search for γ -rays following $\beta\beta$ decay of ^{100}Mo to excited states of ^{100}Ru . *Phys. Lett. B* **1992**, *275*, 506. [[CrossRef](#)]
31. Kidd, M.F.; Esterline, J.H.; Finch, S.W.; Tornow, W. Two-neutrino double- β decay of ^{150}Nd to excited final states in ^{150}Sm . *Phys. Rev. C* **2014**, *90*, 055501. [[CrossRef](#)]
32. Zyla, P.A.; Barnett, R.M.; Beringer, J.; Dahl, O.; Dwyer, D.A.; Groom, D.E.; Lin, C.J.; Lugovsky, K.S.; Pianori, E.; Robinson, D.J.; et al. Particle Data Group, Review of Particle Physics. *Prog. Theor. Exp. Phys.* **2020**, *2020*, 083C01.

33. Kolhinen, V.S.; Eronen, T.; Gorelov, D.; Hakala, J.; Jokinen, A.; Kankainen, A.; Moore, I.D.; Rissanen, J.; Saastamoinen, A.; Suhonen, J.; et al. Double- β decay Q Value ^{150}Nd . *Phys. Rev. C* **2010**, *82*, 022501. [[CrossRef](#)]
34. Artemiev, V.; Brakchman, E.; Karelin, A.; Kirichenko, V.; Klimenko, A.; Kozodaeva, O.; Lubimova, V.; Mitin, A.; Osetrov, A.; Paramokhin, V.; et al. Half-life measurement of ^{150}Nd $2\beta 2\nu$ decay in the time projection chamber experiment. *Phys. Lett. B* **1995**, *345*, 564. [[CrossRef](#)]
35. De Silva, A.; Moe, M.K.; Nelson, M.A.; Vient, M.A. Double β decays of ^{100}Mo and ^{150}Nd . *Phys. Rev. C* **1997**, *56*, 2451. [[CrossRef](#)]
36. Arnold, R.; Augier, C.; Baker, J.D.; Barabash, A.S.; Basharina-Freshville, A.; Blondel, S.; Blot, S.; Bongrand, M.; Brudanin, V.; Busto, J.; et al. Measurement of the $2\nu\beta\beta$ decay half-life of ^{150}Nd and a search for $0\nu\beta\beta$ decay processes with the full exposure from the NEMO-3 detector. *Phys. Rev. D* **2016**, *94*, 072003. [[CrossRef](#)]
37. Barabash, A.S.; Hubert, Ph.; Nachab, A.; Umatov, V.I. Investigation of $\beta\beta$ decay in ^{150}Nd and ^{148}Nd to the excited states of daughter nuclei. *Phys. Rev. C* **2009**, *79*, 045501. [[CrossRef](#)]
38. Blondel, S. Optimisation du Blindage Contre les Neutrons pour le Demonstrateur de SuperNEMO et Analyse de la Double Desintegration Beta du Neodyme-150 vers les Etats Excites du Samarium-150 Avec le Detecteur NEMO-3. Ph.D. Thesis, LAL (Laboratoire de l'Accélérateur Linéaire - Université Paris-Saclay), Orsay, France, 2013.
39. Boiko, R.S. Chemical purification of lanthanides for low-background experiments. *Int. J. Mod. Phys. A* **2017**, *32*, 1743005. [[CrossRef](#)]
40. Polischuk, O.G.; Barabash, A.S.; Belli, P.; Bernabei, R.; Boiko, R.S.; Cappella, F.; Cerulli, R.; Danevich, F.A.; Incicchitti, A.; Laubenstein, M.; et al. Purification of lanthanides for double beta decay experiments. *AIP Conf. Proc.* **2013**, *1549*, 124.
41. Barabash, A.S.; Belli, P.; Bernabei, R.; Boiko, R.S.; Cappella, F.; Caracciolo, V.; Cerulli, R.; Danevich, F.A.; Di Marco, A.; Incicchitti, A.; et al. Double beta decay of ^{150}Nd to the first excited 0_1^+ level of ^{150}Sm : Preliminary results. *Nucl. Phys. Energy* **2018**, *19*, 95. [[CrossRef](#)]
42. Kasperovych, D.V.; Barabash, A.S.; Belli, P.; Bernabei, R.; Boiko, R.S.; Cappella, F.; Caracciolo, V.; Cerulli, R.; Danevich, F.A.; Di Marco, A.; et al. Study of double- β decay of ^{150}Nd to the first 0_1^+ excited level of ^{150}Sm . *AIP Conf. Proc.* **2019**, *2165*, 020014.
43. Polischuk, O.G. Presentation at ICNFP Conference. In Proceedings of the 9th International Conference on New Frontiers in Physics (ICNFP 2020), Athens, Greece, 4 September–2 October 2020.
44. Tretyak, V.I.; Zdesenko, Y.G. Tables of double beta decay data—An update. *At. Data Nucl. Data Tables* **2002**, *80*, 83–116. [[CrossRef](#)]
45. Barabash, A.S. Double beta decay to the excited states: Review. *AIP Conf. Proc.* **2017**, *1894*, 020002.
46. Barabash, A.S. Precise Half-Life Values for Two-Neutrino Double- β Decay: 2020 review. *Universe* **2020**, *6*, 159. [[CrossRef](#)]
47. Meshik, A.P.; Hohenberg, C.M.; Pravdivtseva, O.V.; Kapusta, Y.S. Weak decay of ^{130}Ba and ^{132}Ba : Geochemical measurements. *Phys. Rev. C* **2001**, *64*, 035205. [[CrossRef](#)]
48. Pujol, M.; Marty, B.; Burnard, P.; Philippot, P. Xenon in Archean barite: Weak decay of ^{130}Ba , mass dependent isotopic fractionation and implication for barite formation. *Geochim. Cosmochim. Acta* **2009**, *73*, 6834. [[CrossRef](#)]
49. Gavriilyuk, Y.M.; Gangapshev, A.M.; Kazalov, V.V.; Kuzminov, V.V.; Panasenko, S.I.; Ratkevich, S.S. Indications of $2\nu 2K$ capture in ^{78}Kr . *Phys. Rev. C* **2013**, *87*, 035501. [[CrossRef](#)]
50. Ratkevich, S.S.; Gangapshev, A.M.; Gavriilyuk, Y.M.; Karpeshin, F.F.; Kazalov, V.V.; Kuzminov, V.V.; Panasenko, S.I.; Trzhaskovskaya, M.B.; Yakimenko, S.P. Comparative study of the double-K-shell-vacancy production in single- and double-electron-capture decay. *Phys. Rev. C* **2017**, *96*, 065502. [[CrossRef](#)]
51. Agostini, M.; Allardt, M.; Bakalyarov, A.M.; Balata, M.; Barabanov, I.; Barros, N.; Baudis, L.; Bauer, C.; Bellotti, E.; Belogurov, S.; et al. Limit on the radiative neutrinoless double electron capture of ^{36}Ar from GERDA Phase I. *Eur. Phys. J. C* **2016**, *76*, 652. [[CrossRef](#)]
52. Angloher, G.; Bauer, M.; Bauer, P.; Bavykina, I.; Bento, A.; Bucci, C.; Canonica, L.; Ciemniak, C.; Defay, X.; Deuter, G.; et al. New limits on double electron capture of ^{40}Ca and ^{180}W . *J. Phys. G* **2016**, *43*, 095202. [[CrossRef](#)]
53. Lehnert, B.; Degering, D.; Frotscher, A.; Michel, T.; Zuber, K. A search for the radiative neutrinoless double-electron capture of ^{58}Ni . *J. Phys. G* **2016**, *43*, 065201. [[CrossRef](#)]

54. Belli, P.; Bernabei, R.; Cappella, F.; Cerulli, R.; Danevich, F.A.; d'Angelo, S.; Incicchitti, A.; Kobaychev, V.V.; Poda, D.V.; Tretyak, V.I. Final results of experiment to search for 2β processes in zinc and tungsten with the help of radiopure ZnWO₄ crystal scintillators. *J. Phys. G* **2011**, *38*, 115107. [[CrossRef](#)]
55. Belli, P.; Bernabei, R.; Cappella, F.; Cerulli, R.; Danevich, F.A.; d'Angelo, S.; Incicchitti, A.; Kovtun, G.P.; Kovtun, N.G.; Laubenstein, M.; et al. Search for 2β decays of ⁹⁶Ru and ¹⁰⁴Ru by ultralow-background HPGe γ spectrometry at LNGS: Final results. *Phys. Rev. C* **2013**, *87*, 034607. [[CrossRef](#)]
56. Belli, P.; Bernabei, R.; Brudanin, V.B.; Cappella, F.; Caracciolo, V.; Cerulli, R.; Chernyak, D.M.; Danevich, F.A.; d'Angelo, S.; Di Marco, A.; et al. Search for double- β decay in ¹⁰⁶Cd with an enriched ¹⁰⁶CdWO₄ crystal scintillator in coincidence with four HPGe detectors. *Phys. Rev. C* **2016**, *93*, 045502. [[CrossRef](#)]
57. Barabash, A.S.; Hubert, P.; Marquet, C.; Nachab, A.; Konovalov, S.I.; Perrot, F.; Piquemal, F.; Umatov, V. Improved limits on β^+ EC and ECEC processes in ¹¹²Sn. *Phys. Rev. C* **2011**, *83*, 045503. [[CrossRef](#)]
58. Andreotti, E.; Arnaboldi, C.; Avignone, F.T., III; Balata, M.; Bandac, I.; Barucci, M.; Beeman, J.W.; Bellini, F.; Brofferio, C.; Bryant, A.; et al. Search for β^+ /EC double beta decay of ¹²⁰Te. *Astropart. Phys.* **2011**, *34*, 643. [[CrossRef](#)]
59. Gavriilyuk, Y.M.; Gangapshev, A.M.; Kazalov, V.V.; Kuzminov, V.V.; Panasenko, S.I.; Ratkevich, S.S.; Tekueva, D.A.; Yakimenko, S.P. A technique for searching for the 2K capture in ¹²⁴Xe with a copper proportional counter. *Phys. Nucl.* **2016**, *78*, 1563. [[CrossRef](#)]
60. Bakalyarov, A.; Balysh, A.; Barabash, A.S.; Benes, P.; Briancon, C.; Brudanin, V.; Cermák, P.; Egorov, V.; Hubert, F.; Hubert, P.; et al. Improved Limits on β^- and $\beta^-\beta^-$ Decays of ⁴⁸Ca. *Pisma Zh. Eksp. Teor. Fiz.* **2002**, *76*, 643. [[CrossRef](#)]
61. Barabash, A.S. Limit on $2\beta(0\nu\chi^0)$ -decay of ⁴⁸Ca. *Phys. Lett. B* **1989**, *216*, 257–258. [[CrossRef](#)]
62. Arnquist, I.J.; Avignone, F.T., III; Barabash, A.S.; Barton, C.J.; Bertrand, F.E.; Blalock, E.; Bos, B.; Busch, M.; Buuck, M.; Caldwell, T.S.; et al. The Majorana Demonstrator's Search for Double-Beta Decay of ⁷⁶Ge to Excited States of ⁷⁶Se. *arXiv* **2020**, arXiv:2008.06014.
63. Beeman, J.W.; Bellini, F.; Benetti, P.; Cardani, L.; Casali, N.; Chiesa, D.; Clemenza, M.; Dafinei, I.; Di Domizio, S.; Ferroni, F.; et al. Double-beta decay investigation with highly pure enriched ⁸²Se for the LUCIFER experiment. *Eur. Phys. J. C* **2015**, *75*, 591. [[CrossRef](#)]
64. Barabash, A.S.; Gurriarán, R.; Hubert, F.; Hubert, P.; Reyss, J.L.; Suhonen, J.; Umatov, V.I. Investigation of the $\beta\beta$ decay of ⁹⁶Zr to excited states in ⁹⁶Mo. *J. Phys. G: Nucl. Part. Phys.* **1996**, *22*, 487–496. [[CrossRef](#)]
65. Argyriades, J.; Arnold, R.; Augier, C.; Baker, J.; Barabash, A.S.; Basharina-Freshville, A.; Bongrand, M.; Broudin-Bay, G.; Brudanin, V.; Caffrey, A.J.; et al. Measurement of the two neutrino double beta decay half-life of ⁹⁶Zr with the NEMO-3 detector. *Nucl. Phys. A* **2010**, *847*, 168–179. [[CrossRef](#)]
66. Finch, S.W.; Tornow, W. Search for two-neutrino double- β decay of ⁹⁶Zr to excited states of ⁹⁶Mo. *Phys. Rev. C* **2015**, *92*, 045501. [[CrossRef](#)]
67. Piepke, A.; Beck, M.; Bockholt, J.; Glatting, D.; Heusser, G.; Klapdor-Kleingrothaus, H.V.; Maier, B.; Petry, F.; Schmidt-Rohr, U.; Strecker, H.; et al. Investigation of the $\beta\beta$ decay of ¹¹⁶Cd into excited states of ¹¹⁶Sn. *Nucl. Phys. A* **1994**, *577*, 493–510. [[CrossRef](#)]
68. Barabash, A.S.; Belli, P.; Bernabei, R.; Cappella, F.; Caracciolo, V.; Cerulli, R.; Chernyak, D.M.; Danevich, F.A.; d'Angelo, S.; Incicchitti, A.; et al. Final results of the Aurora experiment to study 2β decay of ¹¹⁶Cd with enriched ¹¹⁶CdWO₄ crystal scintillators. *Phys. Rev. D* **2018**, *98*, 092007. [[CrossRef](#)]
69. Barabash, A.S.; Hubert, P.; Nachab, A.; Konovalov, S.I.; Vanyushin, I.A.; Umatova, V. Search for β^+ EC and ECEC processes in ¹¹²Sn and $\beta^-\beta^-$ -decay of ¹²⁴Sn to the excited states of ¹²⁴Te. *Nucl. Phys. A* **2008**, *807*, 269–281. [[CrossRef](#)]
70. Bellotti, E.; Cattadori, C.; Cremonesi, O.; Fiorini, E.; Liguori, C.; Pullia, A.; Sverzellati, P.P.; Zanotti, L. A Search for Double Beta Decay of ¹²⁸Te and ¹³⁰Te Leading to the First Excited State of Daughter Nuclei. *Europhys. Lett.* **1987**, *3*, 889. [[CrossRef](#)]
71. Arnaboldi, C.; Brofferio, C.; Bucci, C.; Capelli, S.; Cremonesi, O.; Fiorini, E.; Giuliani, A.; Nucciotti, A.; Pavan, M.; Pedretti, M.; et al. A calorimetric search on double beta decay of ¹³⁰Te. *Phys. Lett. B* **2003**, *557*, 167–175. [[CrossRef](#)]
72. Alduino, C.; Alfonso, K.; Artusa, D.R.; Avignone III, F.T.; Azzolini, O.; Banks, T.I.; Bari, G.; Beeman, J.W.; Bellini, F.; Bersani, A.; et al. Double-beta decay of ¹³⁰Te to the first 0⁺ excited state of ¹³⁰Xe with CUORE-0. *Eur. Phys. J. C* **2019**, *79*, 795. [[CrossRef](#)]

73. Bernabei, R.; Belli, P.; Cappella, F.; Cerulli, R.; Montecchia, F.; Incicchitti, A.; Prospero, D.; Dai, C.J. Search for neutrinoless $\beta\beta$ decay in ^{134}Xe . *Phys. Lett. B* **2002**, *527*, 182–186. [[CrossRef](#)]
74. Asakura, K.; Gando, A.; Gando, Y.; Hachiya, T.; Hayashida, S.; Ikeda, H.; Inoue, K.; Ishidoshiro, K.; Ishikawa, T.; Ishio, S.; et al. Search for double-beta decay of ^{136}Xe to excited states of ^{136}Ba with the KamLAND-Zen experiment. *Nucl. Phys. A* **2016**, *946*, 171–181. [[CrossRef](#)]
75. Argyriades, J.; Arnold, R.; Augier, C.; Baker, J.; Barabash, A.S.; Basharina-Freshville, A.; Bongrand, M.; Broudin, G.; Brudanin, V.; Caffrey, A.J.; et al. Measurement of the double- β decay half-life of ^{150}Nd and search for neutrinoless decay modes with the NEMO-3 detector. *Phys. Rev. C* **2009**, *80*, 032501(R). [[CrossRef](#)]
76. Belli, P.; Bernabei, R.; Boiko, R.S.; Cappella, F.; Caracciolo, V.; Cerulli, R.; Danevich, F.A.; Di Marco, A.; Incicchitti, A.; Kropivnyansky, B.N.; et al. First direct search for 2ε and $\varepsilon\beta^+$ decay of ^{144}Sm and $2\beta^-$ decay of ^{154}Sm . *Eur. Phys. J. A* **2019**, *55*, 201. [[CrossRef](#)]
77. Belli, P.; Bernabei, R.; Boiko, R.S.; Cappella, F.; Caracciolo, V.; Cerulli, R.; Danevich, F.A.; Incicchitti, A.; Kropivnyansky, B.N.; Laubenstein, M.; et al. First search for 2ε and $\varepsilon\beta^+$ decay of ^{162}Er and new limit on $2\beta^-$ decay of ^{170}Er to the first excited level of ^{170}Yb . *J. Phys. G: Nucl. Part. Phys.* **2018**, *45*, 095101. [[CrossRef](#)]
78. Belli, P.; Bernabei, R.; Boiko, R.S.; Cappella, F.; Caracciolo, V.; Cerulli, R.; Danevich, F.A.; di Vacri, M.L.; Incicchitti, A.; Kropivnyansky, B.N.; et al. First search for 2ε and $\varepsilon\beta^+$ processes in ^{168}Yb . *Nucl. Phys. A* **2019**, *990*, 64–78. [[CrossRef](#)]
79. Belli, P.; Bernabei, R.; Cappella, F.; Cerulli, R.; Danevich, F.A.; Grinyov, B.V.; Incicchitti, A.; Kobychyev, V.V.; Mokina, V.M.; Nagorny, S.S.; et al. Search for double beta decay of zinc and tungsten with low background ZnWO_4 crystal scintillators. *Nucl. Phys. A* **2009**, *826*, 256–273. [[CrossRef](#)]
80. Danevich, F.A.; Georgadze, A.S.; Kobychyev, V.V.; Kropivnyansky, B.N.; Nikolaiko, A.S.; Ponkratenko, O.A.; Tretyak, V.I.; Zdesenko, S.Y.; Zdesenko, Y.G.; Bizzeti, P.G.; et al. Search for 2β of cadmium and tungsten isotopes: Final results of the Solotvina experiment. *Phys. Rev. C* **2003**, *68*, 035501. [[CrossRef](#)]
81. Belli, P.; Bernabei, R.; Cappella, F.; Cerulli, R.; Danevich, F.A.; d'Angelo, S.; Di Marco, A.; Incicchitti, A.; Kovtun, G.P.; Kovtun, N.G.; et al. First search for double- β decay of ^{184}Os and ^{192}Os . *Eur. Phys. J. A* **2013**, *49*, 24. [[CrossRef](#)]
82. Belli, P.; Bernabei, R.; Cappella, F.; Cerulli, R.; Danevich, F.A.; Di Marco, A.; Incicchitti, A.; Laubenstein, M.; Nagorny, S.S.; Nisi, S.; et al. First search for double- β decay of platinum by ultra-low background HP Ge γ spectrometry. *Eur. Phys. J. A* **2011**, *47*, 91. [[CrossRef](#)]
83. Cerulli, R.; Belli, P.; Bernabei, R.; Cappella, F.; Nozzoli, F.; Montecchia, F.; d'Angelo, A.; Incicchitti, A.; Prospero, D.; Dai, C.J. Performances of a BaF_2 detector and its application to the search for $\beta\beta$ decay modes in ^{130}Ba . *Nucl. Instr. Meth. A* **2004**, *525*, 535–543. [[CrossRef](#)]
84. Belli, P.; Bernabei, R.; Brudanin, V.B.; Cappella, F.; Caracciolo, V.; Cerulli, R.; Danevich, F.A.; Incicchitti, A.; Kasperovych, D.V.; Klavdlienko, V.R.; et al. Search for double beta decay of ^{106}Cd with an enriched $^{106}\text{CdWO}_4$ crystal scintillator in coincidence with CdWO_4 scintillation counters. *Universe* **2020**, *6*, 182. [[CrossRef](#)]
85. Barabash, A.S.; Kuzminov, V.V.; Lobashev, V.M.; Novikov, V.M.; Ovchinnikov, B.M.; Pomansky, A.A. Results of the experiment on the search for double beta decay of ^{136}Xe , ^{134}Xe and ^{124}Xe . *Phys. Lett. A* **1989**, *223*, 273–276. [[CrossRef](#)]
86. Belli, P.; Bernabei, R.; Boiko, R.S.; Cappella, F.; Cerulli, R.; Danevich, F.A.; Incicchitti, A.; Kropivnyansky, B.N.; Laubenstein, M.; Mokina, V.M.; et al. New limits on 2ε , $\varepsilon\beta^+$ and $2\beta^+$ decay of ^{136}Ce and ^{138}Ce with deeply purified cerium sample. *Eur. Phys. J. A* **2017**, *53*, 172. [[CrossRef](#)]
87. Belli, P.; Bernabei, R.; Cappella, F.; Cerulli, R.; Danevich, F.A.; d'Angelo, S.; Di Vacri, M.L.; Incicchitti, A.; Laubenstein, M.; Nagorny, S.S.; et al. First search for double β decay of dysprosium. *Nucl. Phys. A* **2011**, *859*, 126–139. [[CrossRef](#)]
88. Barabash, A.S.; Brudanin, V.B.; Klimenko, A.A.; Konovalov, S.I.; Rakhimov, A.V.; Rukhadze, E.N.; Rukhadze, N.I.; Shitov, Y.A.; Stekl, I.; Warot, G.; et al. Improved limits on $\beta^+\text{EC}$ and ECEC processes in ^{74}Se . *Nucl. Phys. A* **2020**, *996*, 121697. [[CrossRef](#)]
89. Belli, P.; Bernabei, R.; Cerulli, R.; Danevich, F.A.; Galenin, E.; Gektin, A.; Incicchitti, A.; Isaienko, V.; Kobychyev, V.V.; Laubenstein, M.; et al. Radioactive contamination of $\text{SrI}_2(\text{Eu})$ crystal scintillator. *Nucl. Instr. Meth. A* **2012**, *670*, 10–17. [[CrossRef](#)]

90. Belli, P.; Bernabei, R.; Boiko, R.S.; Brudanin, V.B.; Cappella, F.; Caracciolo, V.; Cerulli, R.; Chernyak, D.M.; Danevich, F.A.; d'Angelo, S.; et al. Search for double- β decay processes in ^{106}Cd with the help of a $^{106}\text{CdWO}_4$ crystal scintillator. *Phys. Rev. C* **2012**, *85*, 044610. [CrossRef]
91. Danevich, F.A.; Hult, M.; Kasperovych, D.V.; Kovtun, G.P.; Kovtun, K.V.; Lutter, G.; Marissens, G.; Polischuk, O.G.; Stetsenko, S.P.; Tretyak, V.I. First search for 2ε and $\varepsilon\beta^+$ decay of ^{174}Hf . *Nucl. Phys. A*, **2020**, *996*, 121703. [CrossRef]
92. Finch, S.W.; Tornow, W. Search for neutrinoless double-electron capture of ^{156}Dy . *Phys. Rev. C*, **2015**, *92*, 065503. [CrossRef]
93. Mount, B.J.; Redshaw, M.; Myers, M. Double-beta-decay Q -values of ^{74}Se and ^{76}Ge . *Phys. Rev. C* **2010**, *81*, 032501. [CrossRef]
94. Singh, B. Nuclear data sheets update for $A=76$. *Nucl. Data Sheets* **1995**, *74*, 63. [CrossRef]
95. Beck, M.; Bockholt, J.; Echternach, J.; Heusser, G.; Hirsch, M.; Klapdor-Kleingrothaus, H.V.; Piepke, A.; Strecker, H.; Zuber, K.; Bakalyarov, A.; et al. New half life limits for the $\beta\beta_{2\nu+0\nu}$ decay of ^{76}Ge to the excited states of ^{76}Se from the Heidelberg-Moscow $\beta\beta$ experiment. *Z. Phys. A* **1992**, *343*, 397–400. [CrossRef]
96. The MAJORANA Project a Status Report, Talk Presented by Steve Elliott at the Neutrinos and Dark Matter in Nuclear Physics Conference on 1–4 June 2015, in Jyväskylä, Finland. Available online: <https://www.npl.washington.edu/majorana/sites/sand.npl.washington.edu/majorana/files/documents/presentations/ElliottNDM2015-2.pdf> (accessed on 13 December 2020)
97. Guinn, I.S.; Arnquist, I.J.; Avignone, F.T., III; Barabash, A.S.; Barton, C.J.; Bertrand, F.E.; Bos, B.; Busch, M.; Buuck, M.; Caldwell, T.S.; et al. Results of the MAJORANA DEMONSTRATOR's Search for Double-Beta Decay of ^{76}Ge to Excited States of ^{76}Se . *J. Phys. Conf. Ser.* **2020**, *1468*, 012115. [CrossRef]
98. Ackermann, K.; Agostini, M.; Allardt, M.; Altmann, M.; Andreotti, E.; Bakalyarov, A.M.; Balata, M.; Barabanov, I.; Barnabé Heider, M.; Barros, N.; et al. The GERDA experiment for the search of $0\nu\beta\beta$ decay in ^{76}Ge . *Eur. Phys. J. C* **2013**, *73*, 2330. [CrossRef]
99. Agostini, M.; Bakalyarov, A.M.; Balata, M.; Barabanov, I.; Baudis, L.; Bauer, C.; Bellotti, E.; Belogurov, S.; Belyaev, S.T.; Benato, G.; et al. Upgrade for Phase II of the GERDA experiment. *Eur. Phys. J. C* **2018**, *78*, 388. [CrossRef]
100. Agostini, M.; Allardt, M.; Bakalyarov, A.M.; Balata, M.; Barabanov, I.; Barros, N.; Baudis, L.; Bauer, C.; Becerici-Schmidt, N.; Bellotti, E.; et al. $2\nu\beta\beta$ decay of ^{76}Ge into excited states with GERDA Phase I. *J. Phys. G: Nucl. Part. Phys.* **2015**, *42*, 115201.
101. Redshaw, M.; Mount, B.J.; Meyers, E.G.; Avignone, F.T., III. Masses of ^{130}Te and ^{130}Xe and Double- β -Decay Q Value of ^{130}Te . *Phys. Rev. Lett.* **2009**, *102*, 212502. [CrossRef]
102. Scielzo, N.D.; Caldwell, S.; Savard, G.; Clark, J.A.; Deibel, C.M.; Fallis, J.; Gulick, S.; Lascar, D.; Levand, A.F.; Li, G.; et al. Double- β -Decay Q values of ^{130}Te , ^{128}Te , and ^{120}Te . *Phys. Rev. C* **2009**, *80*, 025501. [CrossRef]
103. Rahaman, S.; Elomaa, V.V.; Eronen, T.; Hakala, J.; Jokinen, A.; Kankainen, A.; Rissanen, J.; Suhonen, J.; Weber, C.; Äystö, J. Double-beta decay Q values of ^{116}Cd and ^{130}Te . *Phys. Lett. B* **2011**, *703*, 412. [CrossRef]
104. Andreotti, E.; Arnaboldi, C.; Avignone, F.T., III; Balata, M.; Bandac, I.; Barucci, M.; Beeman, J.W.; Bellini, F.; Brofferio, C.; Bryant, A.; et al. Search for double- β decay of ^{130}Te to the first 0^+ excited state of ^{130}Xe with the CUORICINO experiment bolometer array. *Phys. Rev. C* **2012**, *85*, 045503. [CrossRef]
105. Fehr, M.A.; Rehkämper, M.; Halliday, A.N. Application of MC-ICPMS to the precise determination of tellurium isotope compositions in chondrites, iron meteorites and sulfides. *Int. J. Mass Spectrom.* **2004**, *232*, 83. [CrossRef]
106. Haller, E.E. Physics and design of advanced IR bolometers and photoconductors. *Infrared Phys.* **1985**, *25*, 257. [CrossRef]
107. Alduino, C.; Alfonso, K.; Artusa, D.R.; Avignone, F.T., III; Azzolini, O.; Balata, M.; Banks, T.I.; Bari, G.; Beeman, J.W.; Bellini, F.; et al. CUORE-0 detector: Design, construction and operation. *J. Inst.* **2016**, *11*, P07009. [CrossRef]
108. Alfonso, K.; Artusa, D.R.; Avignone, F.T., III; Azzolini, O.; Balata, M.; Banks, T.I.; Bari, G.; Beeman, J.W.; Bellini, F.; Bersani, A.; et al. Search for Neutrinoless Double-Beta Decay of ^{130}Te with CUORE-0. *Phys. Rev. Lett.* **2015**, *115*, 102502. [CrossRef]
109. Alduino, C.; Alfonso, K.; Artusa, D.R.; Avignone, F.T., III; Azzolini, O.; Banks, T.I.; Bari, G.; Beeman, J.W.; Bellini, F.; Bersani, A.; et al. Analysis techniques for the evaluation of the neutrinoless double- β decay lifetime in ^{130}Te with the CUORE-0 detector. *Phys. Rev. C* **2016**, *93*, 045503. [CrossRef]

110. Barabash, A.S.; Hubert, F.; Hubert, P.; Umatov, V.I. New limits on the $\beta\beta$ decay of ^{130}Te to excited states of ^{130}Xe . *Eur. Phys. J. A* **2001**, *11*, 143–145. [[CrossRef](#)]
111. Kawrakow, I.; Mainegra-Hing, E.; Rogers, D.W.O.; Tessier, F.; Walters, B.R.B. *The EGSnrc Code System: Monte Carlo Simulation of Electron and Photon Transport*; NRCC (National Research Council Canada) Report PIRS-701; NRCC: Ottawa, ON, Canada, 2003.
112. Agostinelli, S.; Allison, J.; Amako, K.; Apostolakis, J.; Araujo, H.; Arce, P.; Asai, M.; Axen, D.; Banerjee, S.; Barrand, G.; et al. GEANT4—a simulation toolkit. *Nucl. Instr. Meth. A* **2003**, *506*, 250. [[CrossRef](#)]
113. Boswell, M.; Chan, Y.D.; Detwiler, J.A.; Finnerty, P.; Henning, R.; Gehman, V.M.; Johnson, R.A.; Jordan, D.V.; Kazkaz, K.; Knapp, M.; et al. MaGe-a Geant4-Based Monte Carlo Application Framework for Low-Background Germanium Experiments. *IEEE Trans. Nucl. Sci.* **2011**, *58*, 1212–1220. [[CrossRef](#)]
114. Allison, J.; Amako, K.; Apostolakis, J.; Araujo, H.; Arce Dubois, P.; Asai, M.; Barrand, G.; Capra, R.; Chauvie, S.; Chytracsek, R.; et al. Geant4 developments and applications. *IEEE Trans. Nucl. Sci.* **2006**, *53*, 270–278. [[CrossRef](#)]
115. Ponkratenko, O.A.; Tretyak, V.I.; Zdesenko, Y.G. Event generator DECAY4 for simulating double-beta processes and decays of radioactive nuclei. *Phys. At. Nucl.* **2000**, *63*, 1282. [[CrossRef](#)]
116. Tretyak, V.I. (Institute for Nuclear Research of NASU, Kyiv, Ukraine). Personal communication, 2007.
117. Belli, P.; Bernabei, R.; d’Angelo, S.; Cappella, F.; Cerulli, R.; Incicchitti, A.; Laubenstein, M.; Prosperi, D.; Tretyak, V.I. First limits on neutrinoless resonant 2ϵ captures in ^{136}Ce and new limits for other 2β processes in ^{136}Ce and ^{138}Ce isotopes. *Nucl. Phys. A* **2009**, *824*, 101. [[CrossRef](#)]
118. Belli, P.; Bernabei, R.; Boiko, R.S.; Cappella, F.; Cerulli, R.; Danevich, F.A.; Incicchitti, A.; Kropivyansky, B.N.; Laubenstein, M.; Poda, D.V.; et al. Search for double beta decay of ^{136}Ce and ^{138}Ce with HPGe gamma detector. *Nucl. Phys. A* **2014**, *930*, 195. [[CrossRef](#)]
119. Belli, P.; Bernabei, R.; Cappella, F.; Cerulli, R.; Danevich, F.A.; d’Angelo, S.; Incicchitti, A.; Laubenstein, M.; Polischuk, O.G.; Prosperi, D.; et al. Search for double beta decays of ^{96}Ru and ^{104}Ru by ultra-low background HPGe gamma spectrometry. *Eur. Phys. J. A* **2009**, *42*, 171. [[CrossRef](#)]
120. Belli, P.; Bernabei, R.; Incicchitti, A.; Arpesella, C.; Kobaychev, V.V.; Ponkratenko, O.A.; Tretyak, V.I.; Zdesenko, Y.G. New limits on $2\beta^+$ decay processes in ^{106}Cd . *Astropart. Phys.* **1999**, *10*, 115–120. [[CrossRef](#)]
121. Das, S.; Ghorui, S.K.; Raina, P.K.; Singh, A.K.; Rath, P.K.; Cappella, F.; Cerulli, R.; Laubenstein, M.; Belli, P.; Bernabei, R. Preliminary study of feasibility of an experiment looking for excited state double beta transitions in tin. *Nucl. Instr. Meth. A* **2015**, *797*, 130. [[CrossRef](#)]
122. Pirinen, P.; Suhonen, J. Systematic approach to β and $2\nu\beta\beta$ decays of mass $A = 100 - 136$ nuclei. *Phys. Rev. C* **2015**, *91*, 054309. [[CrossRef](#)]
123. Fantini, G. Presentation of Its PhD Thesis. Available online: https://indico.gssi.it/event/131/contributions/350/attachments/169/248/FANTINI_Guido_PhDseminar_v1_FINAL.pdf (accessed on 13 December 2020).

Publisher’s Note: MDPI stays neutral with regard to jurisdictional claims in published maps and institutional affiliations.



© 2020 by the authors. Licensee MDPI, Basel, Switzerland. This article is an open access article distributed under the terms and conditions of the Creative Commons Attribution (CC BY) license (<http://creativecommons.org/licenses/by/4.0/>).